Circulation of Matter

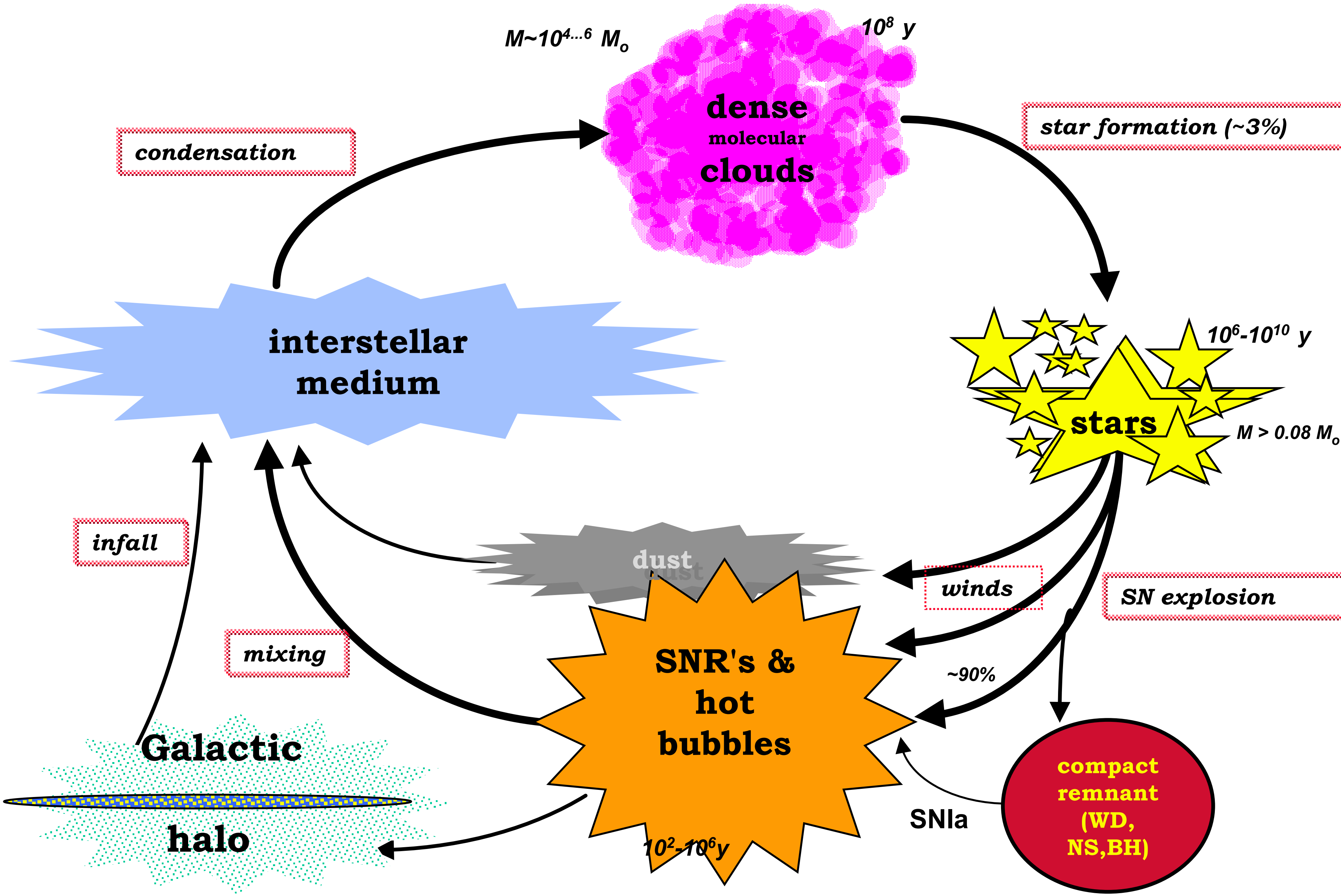

Roland Diehl

Cosmic Matter Cycling

- **Stages, Sub-Topics:**
  - ☆ Interstellar Gas, forming Stars
    - ☞ ISM Phases, Cloud Condensation
    - ☞ Protostellar Collapse, Protostars
  - ☆ Stars
    - ☞ Mass Function(s)
    - ☞ Stellar Evolution, Lifetimes
    - ☞ Mass Loss: Winds, Binaries, Novae, Supernovae
  - ☆ Remnants
    - ☞ Supernova Remnants
    - ☞ ISM Bubbles and Superbubbles, Mixing
    - ☞ Compact Remnants
  - ☆ Chemical Evolution
    - ☞ Galactic Gas and Stars
    - ☞ Chemical Elements
    - ☞ Cosmic Star Formation

The Interstellar Medium

- **Masses**
  - ☆ Galaxy/ISM/ISM gas:
    $1\ 10^{12}\ M_\odot / 1.4\ 10^{11}\ M_\odot / 4\ 10^{9}\ M_\odot$
- **Components**
  - ☆ Diffuse ISM
    - ☞ Hot Gas (T> 10^6K; plasma)
    - ☞ Warm Ionized Gas (T~ 10^4K; e^-,ions)
    - ☞ Cold Gas (T~10-100K; neutral)
    - ☞ Dust
    - ☞ Cosmic Rays
  - ☆ Clouds & Prominent Regions
    - ☞ Diffuse Clouds
    - ☞ Molecular Clouds
      - **Giant Molecular Clouds (GMC)**
      - **Dark Clouds**
    - ☞ HII Regions
    - ☞ SNR, Superbubbles

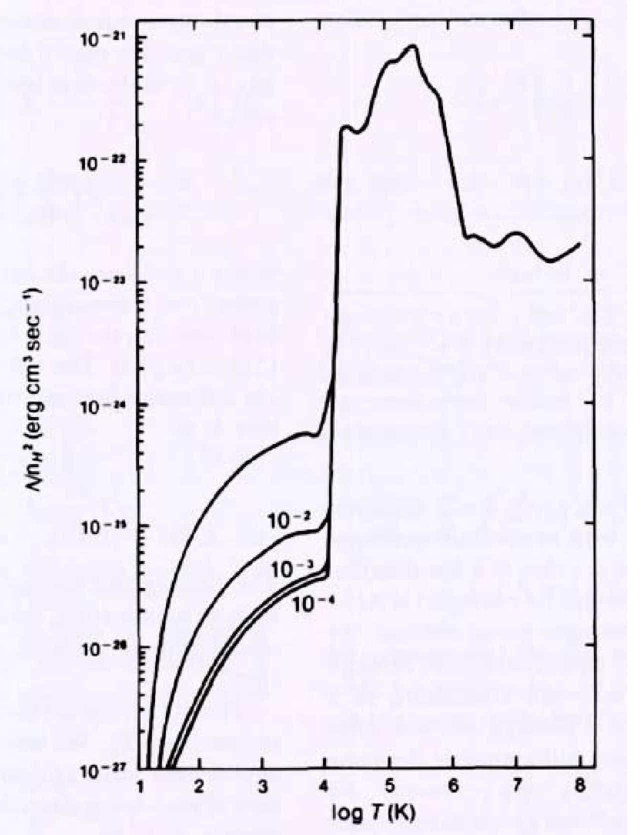

Figure 18.4. Cooling function for interstellar gas. For $T < 10^4$ K, different curves correspond to different values of n_e/n_H. For $T > 10^4$,

$$\tau_{\rm cool} = \frac{3/2 N k_B T}{\Gamma - \Lambda}$$

Roland Diehl

Views of the ISM

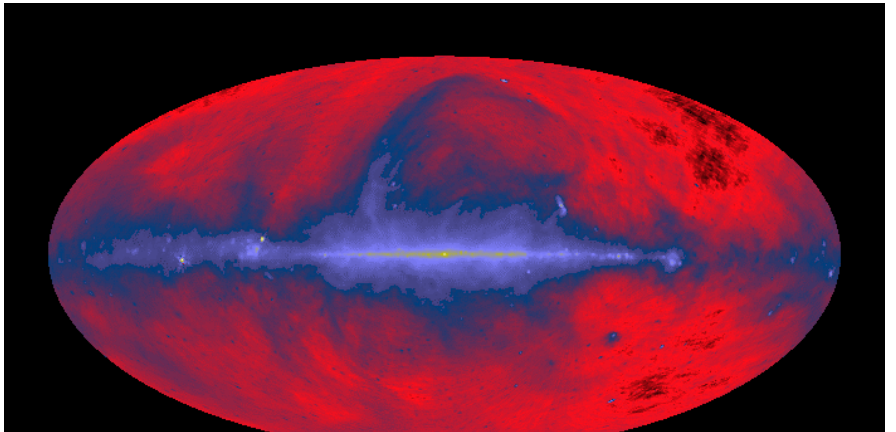
408 MHz Radio Synchrotron Emission: electrons

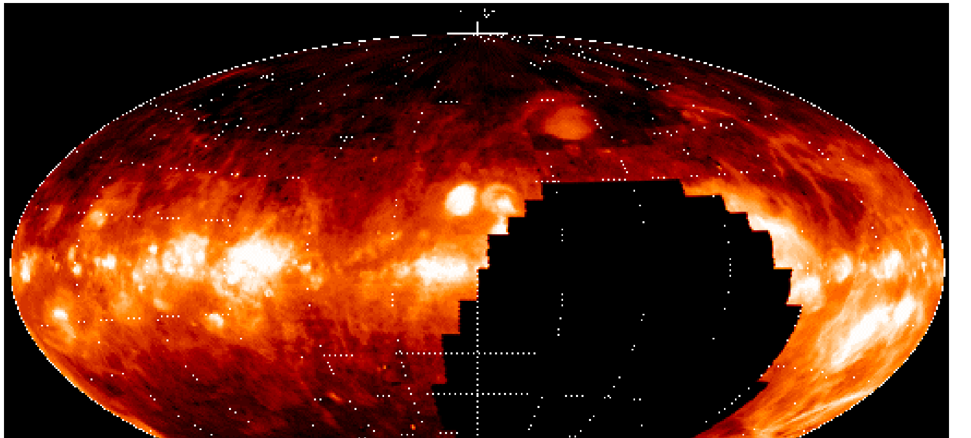
Hα Emission: ionized gas (WHAM)

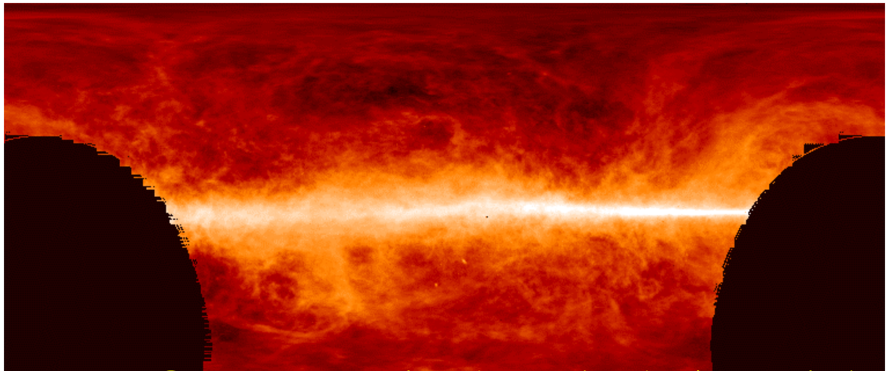
21cm H Emission: neutral Hydrogen (Leiden/Dwingeloo)

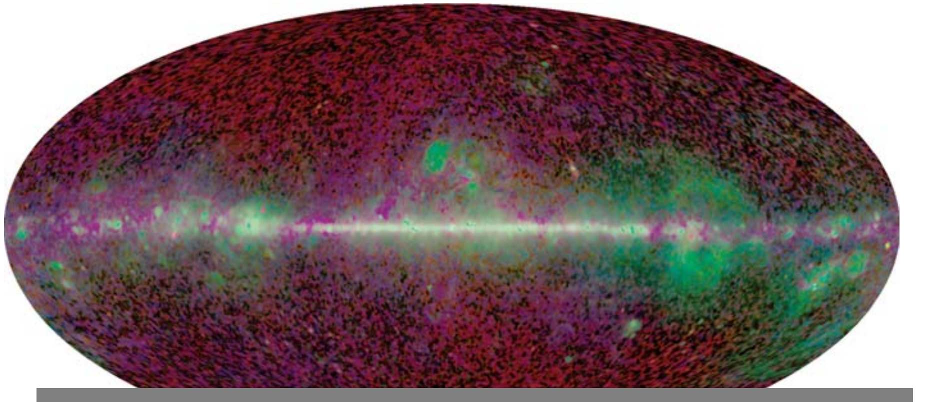
Radio Emission: dust(b), electrons (r-sync,g-ff) (WMAP)



Starlight (COBE 3μm, optical)

- **Disk-like plus Patchy Localized Structures & Filaments (z~500pc)**
- **HI:** $\langle n_n \rangle(Z) = (0.57\ \mathrm{cm}^{-3}) \left\{ 0.70\ \exp\left[-\left(\frac{Z}{127\ \mathrm{pc}}\right)^2\right] + 0.19\ \exp\left[-\left(\frac{Z}{318\ \mathrm{pc}}\right)^2\right] + 0.11\ \exp\left(-\frac{|Z|}{403\ \mathrm{pc}}\right) \right\}$

Views of Clouds of the ISM

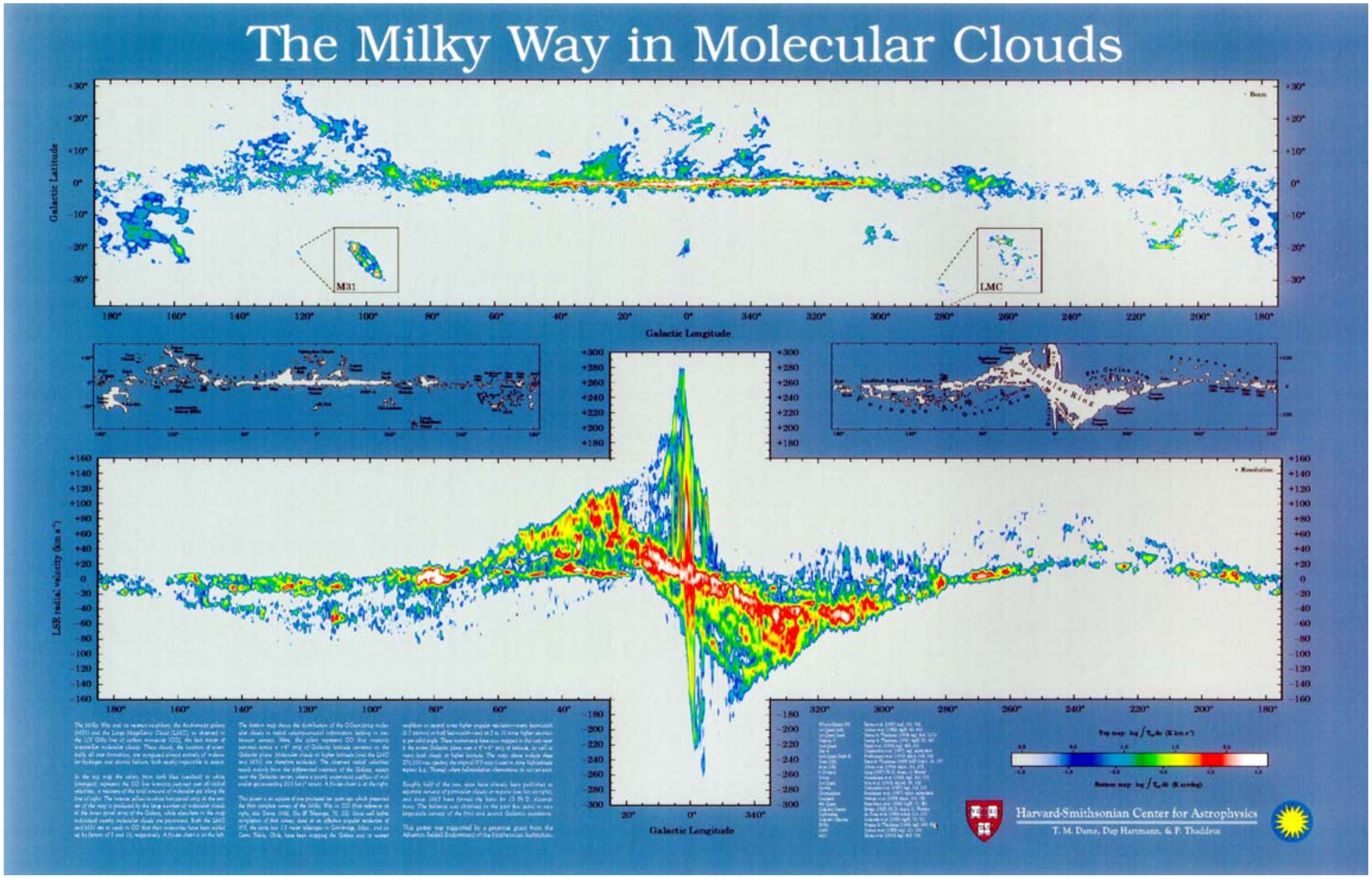

- Molecular Clouds are Confined to a Narrow Disk (z~50pc)

Roland Diehl

HII Regions, Ionized Gas

- **Ionizing HE Part of Starlight Creates "Strömgren Sphere"**

$$r_S = (30\ \mathrm{pc}) \left(\frac{N_{48}}{n_\mathrm{H}\ n_e} \right)^{\frac{1}{3}}$$

where N_{48} is the number of ionizing photons emitted per unit time by the central star, in $10^{48}\ \mathrm{s}^{-1}$ (e.g., $N_{48} \simeq 34$ for an O5V star and $N_{48} \simeq 1.7$ for a B0V star; Vacca *et al.*, 1996), and n_H and n_e are the free-proton and free-electron number densities in the H II region, in cm^{-3} (Spitzer, 1978, p. 109).

- **Radiation ~ "Emission Measure" EM**
  - Free-Free Emission
  - Recombination Radiation (e.g.Hα Emission)

$$\mathrm{EM} = \int n_e^2\ ds$$

$$\langle n_e \rangle (Z) = (0.015\ \mathrm{cm}^{-3})\ \exp\left(-\frac{|Z|}{70\ \mathrm{pc}} \right) + (0.025\ \mathrm{cm}^{-3})\ \exp\left(-\frac{|Z|}{900\ \mathrm{pc}} \right)$$

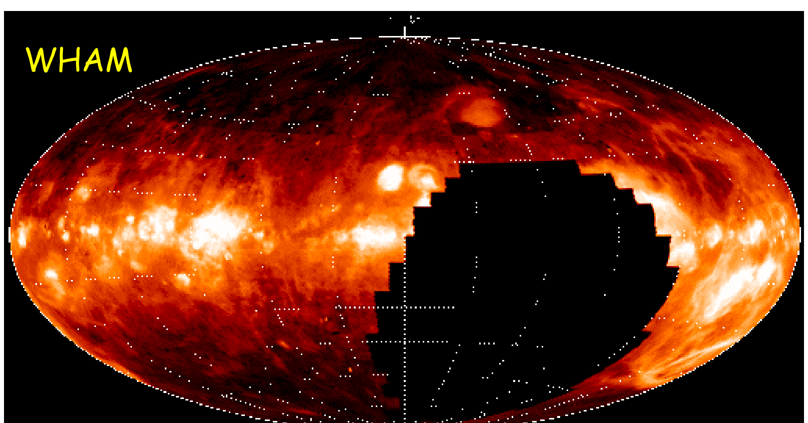

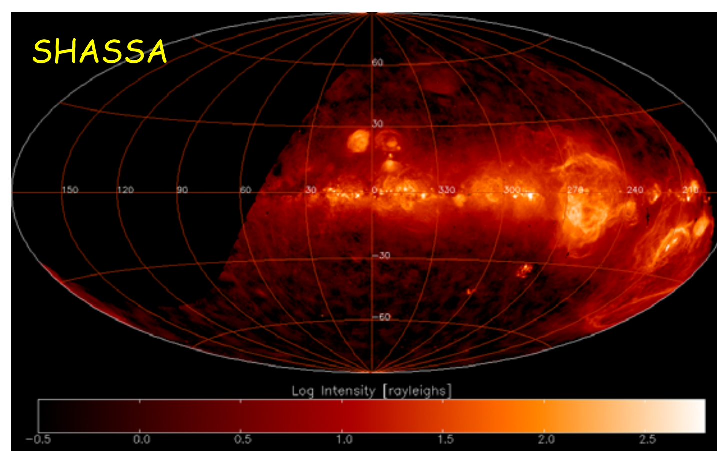

HII Regions: Heating and Cooling

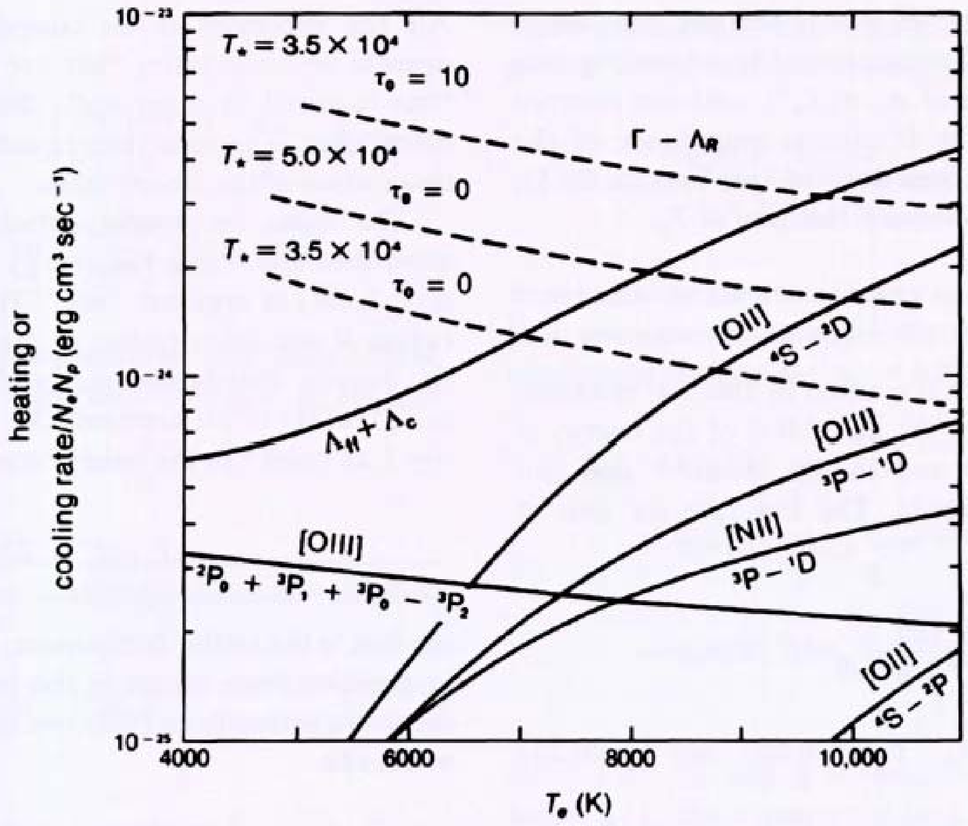

Figure 20.4. Heating and cooling rates versus temperature. Dashed curves give $\Gamma - \Lambda_R$ for three stellar input spectra (T_* denotes the spectral temperature), and τ_o is the optical depth of the medium at the ionization limit. The radiative cooling curve is labeled $\Lambda_R + \Lambda_c$. dominant contributions to the radiative cooling are shown by the light solid curves.

- Temperature Dependency of Heating and Cooling Processes

Hot Plasma

- **T >> 6000K**
  - ☞ Matter Ionized: Ions and Electrons
  - ☞ Processes:
    - Coulomb Scatterings
    - Bremsstrahlung / Free-Free Radiation
    - Recombinations / Ionizations
    - Comptonization / Compton Scattering
  - ☞ Thermal and Non-Thermal Particle Populations (->Radiation Components)

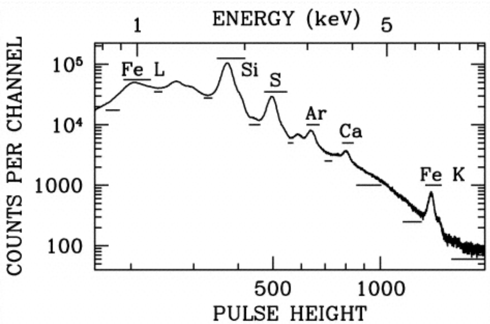

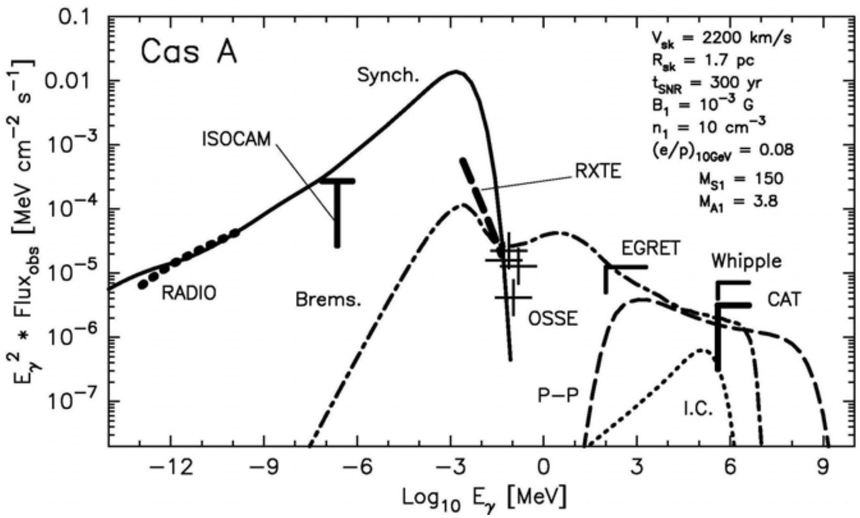

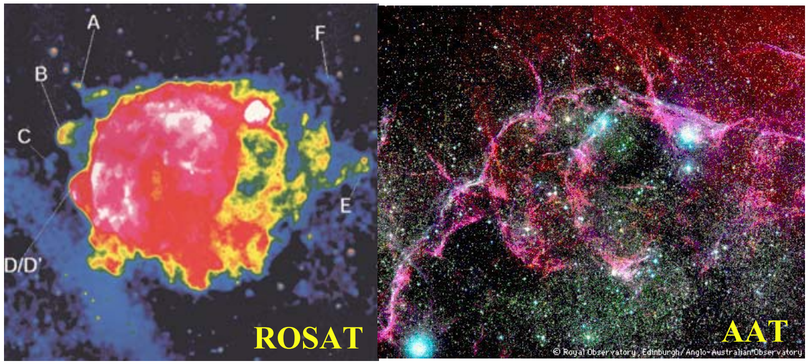

Supernovae and Supernova Remnants

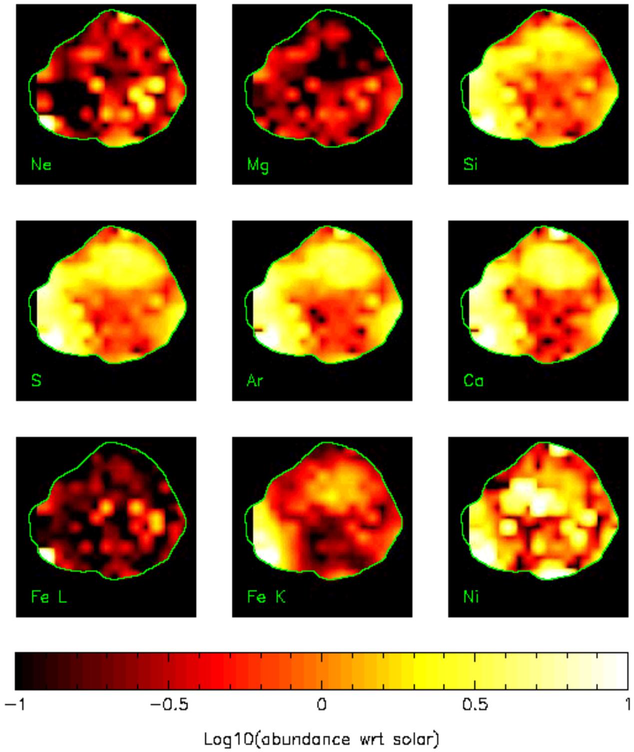

Fig. 5. Abundance maps for the elements included in the spectral fitting. All are plotted on the logarithmic scale indicated by the bar at the bottom.

Cas A / XMM

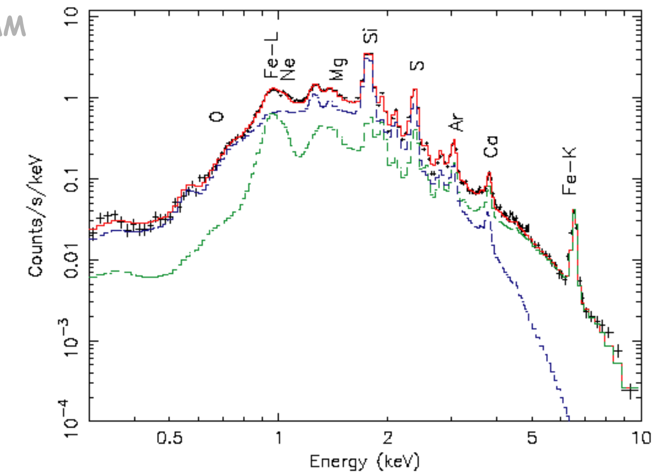

Fig. 2. An example of a spectral fit within a single 20″ × 20″ pixel – cool component in blue, hot component in green and full model in red.

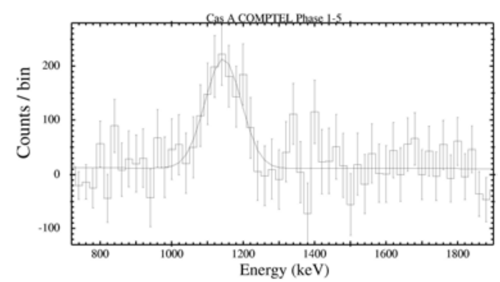

Cas A ^{44}Ti (τ~89y) / COMPTEL

- Prompt SN Light from Radioactivity
- SN Debris Reflects Nucleosynthesis (and Collapsing-Star Structure)
- Interaction of Blast Wave with ISM Results in Shocked Gas & Recombination Radiation
- SNR Radiation Dominated by CSM,ISM Interactions ($M_{swept-up}$>M_{ejecta})

Local ISM Morphology

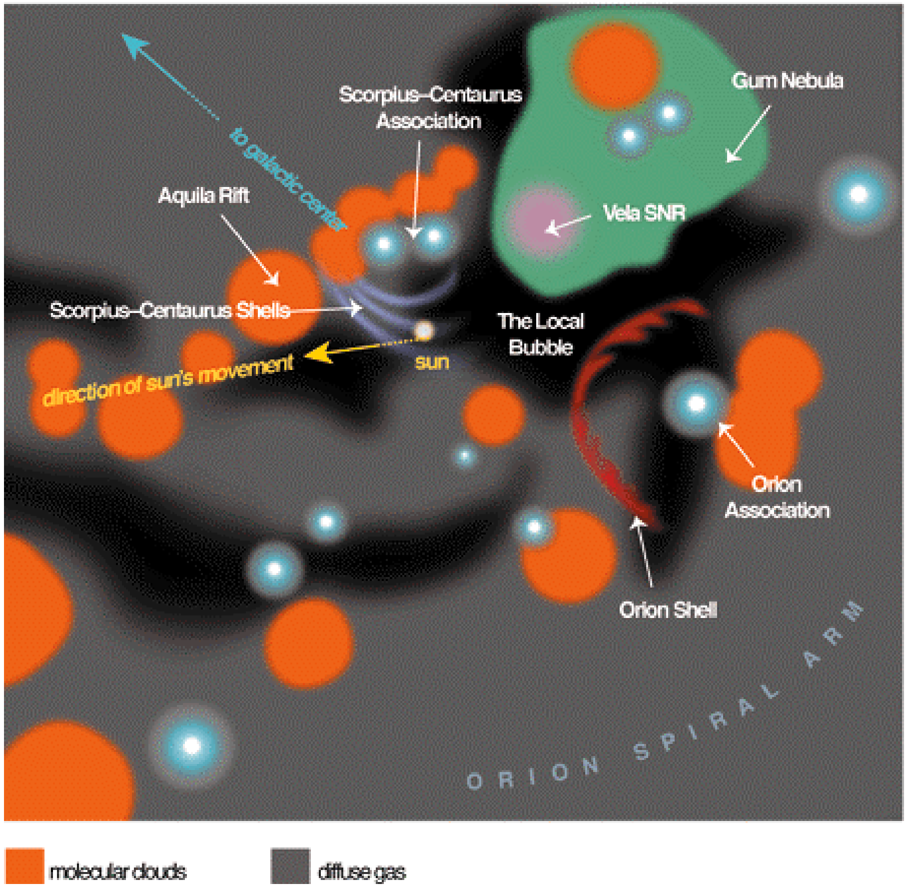

- **Massive Stars Shape ISM, Low-Mass Stars are Embedded**
  - ☞ OB Associations
  - ☞ Swept-Up Shells, Cooling Cavities

Roland Diehl

The Local Bubble

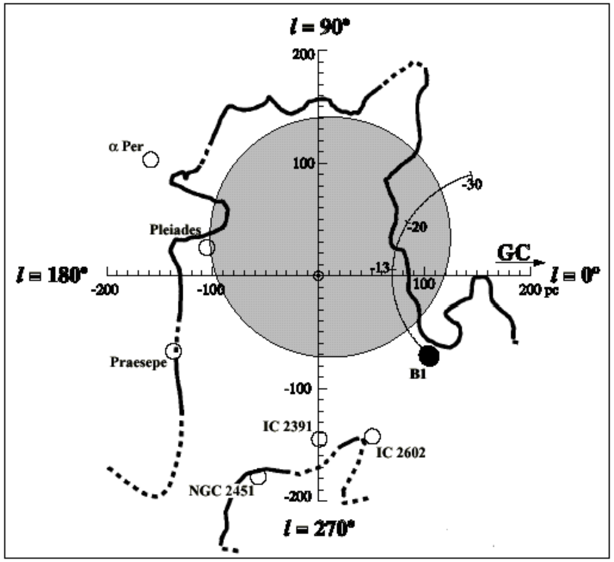

Fig. 2. Sketch of the solar neighborhood seen from above the galactic plane. The center of mass position of Pleiades subgroup B1 is labeled with "B1". The solid line, ending at the actual position of B1, provides the trajectory of the moving group during the past 30 Myrs in the epicyclic approximation (see Sect. 3); center of mass positions 13, 20, and 30 Myrs ago are labeled with -13, -20, and -30. Approximately 13 Myrs ago the most massive B1 star(s) ($M \approx 20\ M_\odot$) must have exploded. The local cavity contours as derived from NaI absorption line studies by Sfeir et al. (1999) are shown as thick solid lines (dashed lines denote directions of uncertain local cavity borders). As can be seen, existing B1 member stars (or at least some of them, given their spatial spread) should have crossed the region, which now forms the Local Bubble.

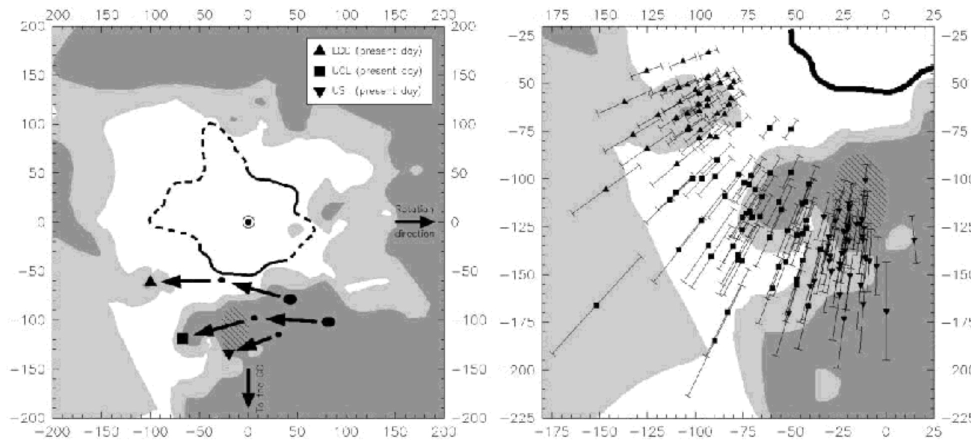

FIG. 1.—*Left*: Local cavity and LB in the plane of the Galactic equator. The filled contours show the Na I distribution (Sfeir et al. 1999), with white used for low-density regions and dark gray for high-density ones. The black contour shows the present size of the LB as determined from X-ray data (Snowden et al. 1998), with the dashed lines indicating contaminated areas where the limits of the LB cannot be accurately determined. The hatched ellipse shows the approximate position of the Ophiuchus molecular cloud (de Geus et al. 1989; Loren 1989a, 1989b). The present and past *x*- and *y*-coordinates of the center of the three subgroups of the Sco-Cen association are shown. For LCC and UCL, the past positions shown are those of 5 and 10 Myr ago, while for US only the position of 5 Myr ago is shown. The dimensions of the filled ellipses indicate the uncertainties in the past positions. Coordinates are expressed in units of parsecs. *Right*: Blowup of the left panel with the present positions of the OB stars in each of the three subgroups. Only those stars with accurately determined positions are shown. The symbol used in each case indicates the subgroup membership using the code established in the left panel.

- Size and Density Inferred from Na Absorption in Spectra of Nearby Stars (Sfeir et al. 1999) and Soft X-ray Shadowing from Nearby Clouds (Snowdon et al. 1998); r~100 pc, n~5 10^{-3} cm^{-3}, T~10^6K
- Origin Attributed to Sco-Cen Association Supernovae (Maiz-Apellaniz 2001) or Pleiades Supernovae (Berghöfer & Breitschwerdt 2002)

Galaxy Disk & Halo: High-Velocity Clouds

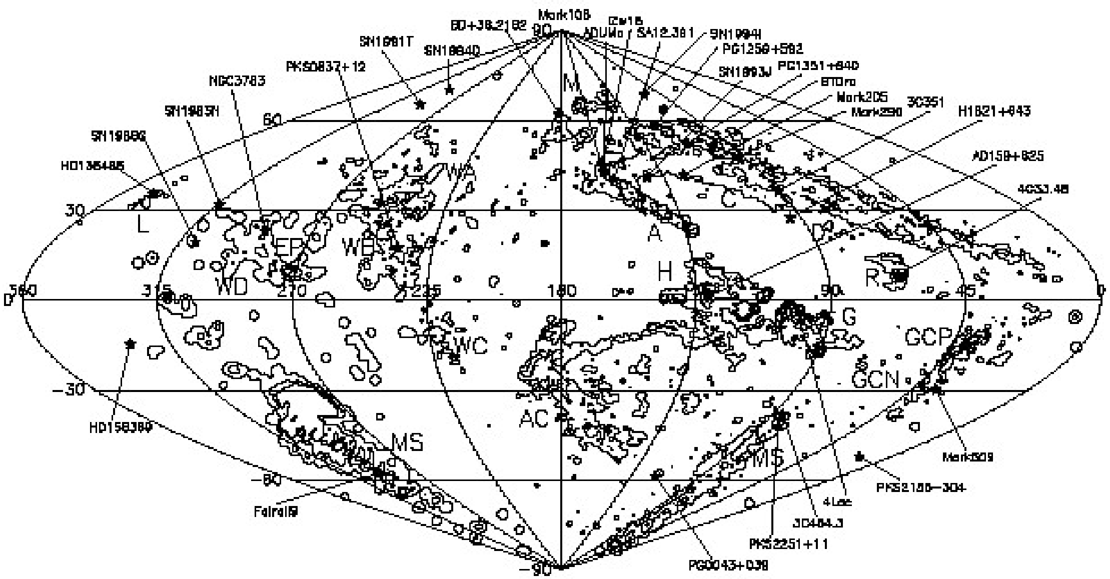

Figure 1 Brightness temperature map of HVCs (HI with $|v_{LSR}| > 90$ km/s). Contours at 0.04, 0.5, and 1.5K. Common names of some complexes are indicated. Background sources in which high-velocity absorption has been detected or claimed are indicated (see Table 3, Table 4, and Section 4).

- **Neutral-Gas Clouds with Large Latitudinal Velocities**
  - ☆ Define: HVC = > 90 km s-1 (LSR)
  - ☆ Typical M~10^5 $M_\odot$, -> E_{kin}~10^{52} erg

☞ Wakker & vanWoerden, 1997

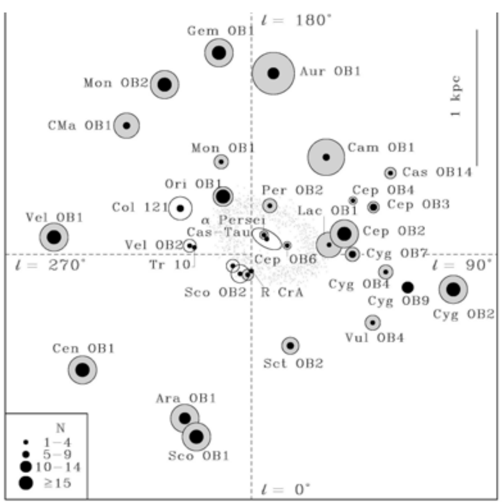

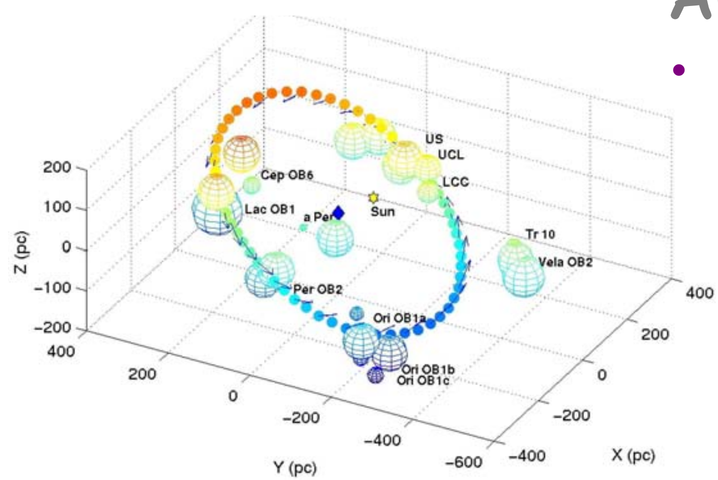

Application:

- **Gould Belt System of OB Associations: From Impact of HVC?**
  - ☞ Oscillation around Disk Gravitational Well
  - ☞ Triggered Star Formation

Roland Diehl

ISM Morphology

No. 1, 1977 THEORY OF ISM 159

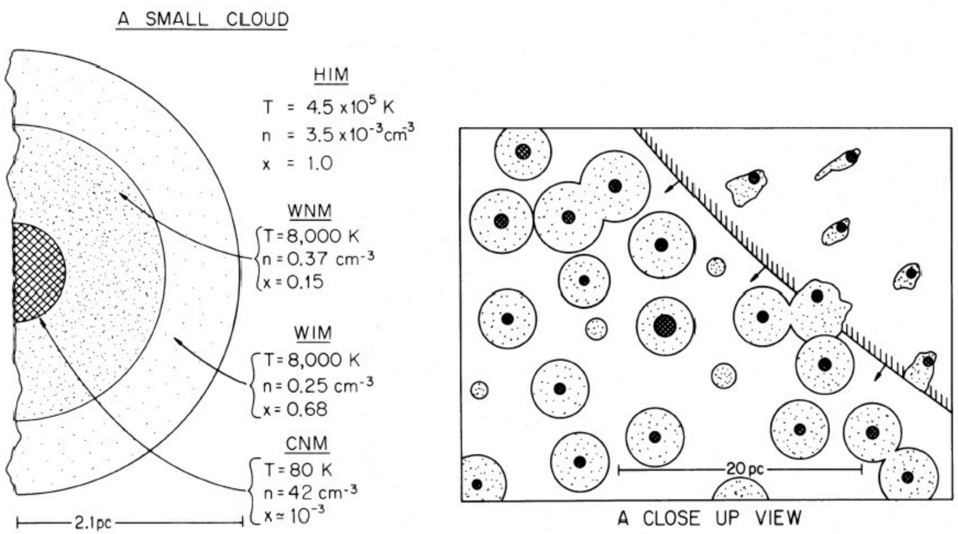

FIG. 1 FIG. 2

FIG. 1.—Cross section of a characteristic small cloud. The crosshatched region shows the cold core, which gives the usual optical absorption lines. Next is the warm neutral medium (WNM) with ionization produced by soft X-ray background. The outer layer (WIM) is gas largely ionized by stellar UV background. Typical values of hydrogen density n, temperature T, and ionization $x = n_e/n$ are shown for each component, except that a higher than average value of the soft X-ray flux has been assumed in order to produce a significant amount of WNM at this pressure.

FIG. 2.—Small-scale structure of the interstellar medium. A cross section of a representative region 30 pc × 40 pc in extent is shown, with the area of the features being approximately proportional to their filling factors. A supernova blast wave is expanding into the region from the upper right. The radius of the neutral cores of the clouds (represented by crosshatching) ranges from about 0.4 to 1 pc in this small region; all the clouds with cores have warm envelopes (*dotted regions*) of radius $a_w \sim 2.1$ pc. A few clouds are too small to have cores. The envelopes of clouds inside the SNR are compressed and distorted.

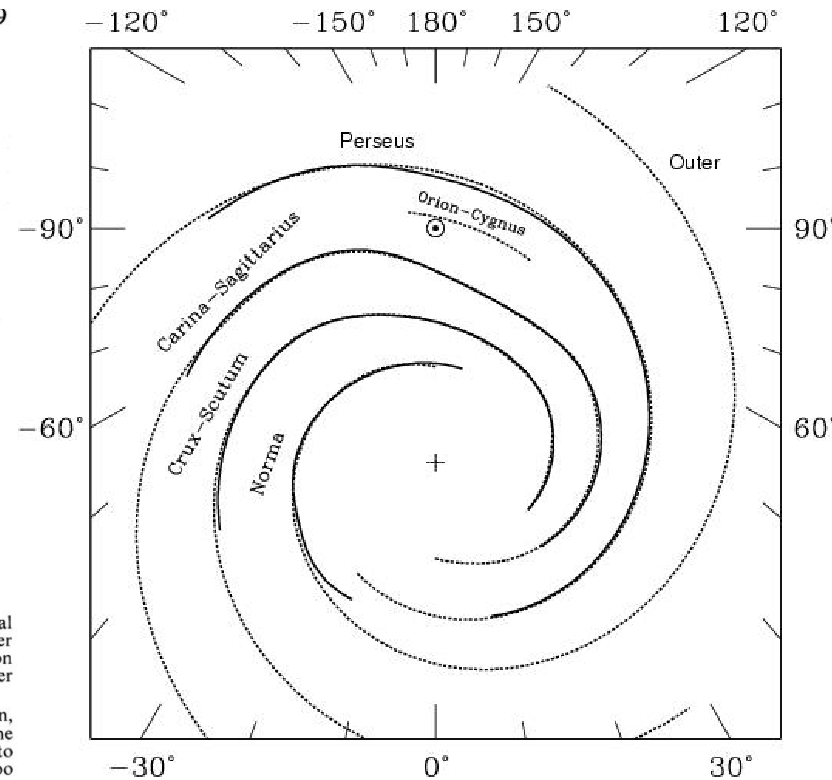

- **Pressure Equilibrium among Phases**
- **Energy Flow:**
  - ☆ Injection by Winds, SNae, Radiation
  - ☆ Dissipation by Cooling

☞ Ostriker & Mc Kee (1977; …)

- **Small-Scale Structure:**
  - ➢ Ionization, CR/Radiative/ Turbulence Heating, and Cooling Processes
  - ➢ Cavities, Shells, Filaments
- **Large-Scale Structure**
  - ➢ Turbulence, Magnetic Field Interactions, Density Waves

Roland Diehl

Constituents of the ISM

constituents of ISM in Milky Way	where	temperature density ...	how observed
atomic hydrogen HI	in disk, some in halo ≈ 90% of mass, 50% of vol.	$50 \ldots 300$K $1 \ldots 100$cm^{-3}	21cm radio line UV absorption lines
molecular hydrogen H_2	dark clouds in disk ≈ 10% of mass, 1% of vol.	$3 \ldots 100$K $10^2 \ldots 10^6$cm^{-3}	UV absorption lines IR emission lines
other molecules CO, HCN, H_2O ...	dark clouds in disk	$3 \ldots 100$K $10^2 \ldots 10^6$cm^{-3}	radio and IR emission
ionized hydrogen HII	near hot stars, emission nebulae	$5000 \ldots 10000$K $10^2 \ldots 10^4$cm^{-3}	optical and IR emission lines, radio continuum
hot gas	everywhere	$10^6 \ldots 10^7$K 0.01cm^{-3}	X-ray emission
dust grains	mostly in disk ≈ 1% of mass	$20 \ldots 100$K size ≈ 2000Å	reddening/absorption of starlight, IR emission
magnetic fields	everywhere	μGauss	polarization of stars, Zeeman effect, synchrotron radiation
cosmic rays	everywhere	energies up to 10^{20}eV	air showers

- **ISM Fraction of Total Galactic Mass: ~15% (typical for spiral galaxies)**

Forming Stars…

- … is not easy
  - ☆ Angular Momentum Must Be Dissipated
  - ☆ Density of Nuclear-Burning Must Be Reached
    - ☞ Fragmentation
    - ☞ Formation of Planets
    - ☞ Bipolar Outflows

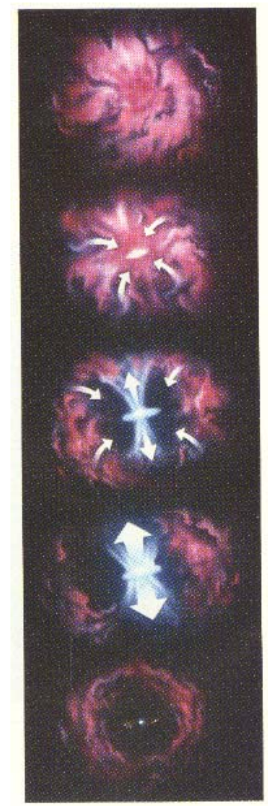

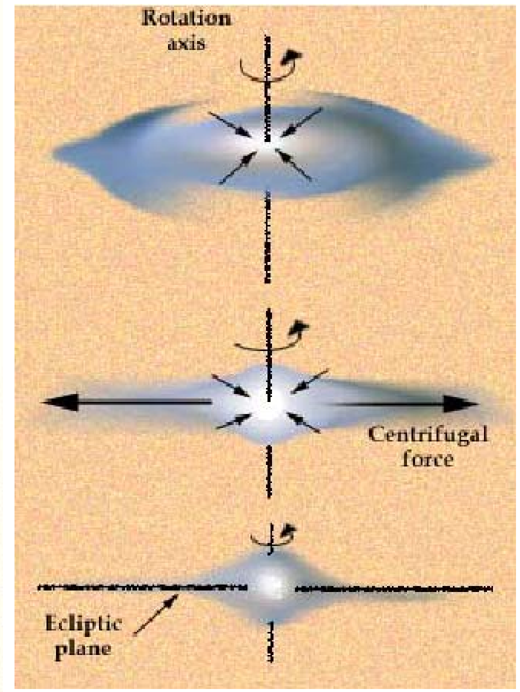

Roland Diehl

Stellar Masses

- Present-Day Mass Function = Observable
  - ☞ Brightness Distribution $N(M_V)$, Scale Height h

$$PDMF(\log m) = \frac{dN}{dM_V}\frac{dM_V}{d(\log m)} 2h(M_V)$$

- "Initial Mass Function"
  - ☞ Use Stellar Lifetimes τ, Star Formation Rate ϕ, Age of Galaxy T

$$IMF = PDMF / \left(T\left\langle \phi(t)\right\rangle\right) = PDMF / \left\{\tau(m)\phi(T)\right\} \approx PDMF / \int_{T-\tau_{ms}}^{T} \phi(t)dt$$

  - ☞ Normalize

Cosmic Rays: Accelerated ISM Particles

- **Accelerating Environments**
  - ☆ Electrostatic Fields
    - ☞Pulsars
  - ☆ Magnetic Fields
    - ☞Near Compact Stars -> … ~10^{13}G
    - ☞In Stellar Environments & SNae -> … ~ G
    - ☞Galactic and Intergalactic Space -> … ~μG
    - ☞Turbulent Magnetic Fields in Shocked Gas
      - Jets (AGN, … , GRB?)
      - SNR
- **Processes**
  - ☆ Fermi II
    - ☞Scattering on "Magnetic Mirrors", e.g., Interstellar Clouds at Random Motion
  - ☆ Fermi I
    - ☞Scattering on Magnetic-Field Turbulences on Both Sides of Shocked-Gas Region

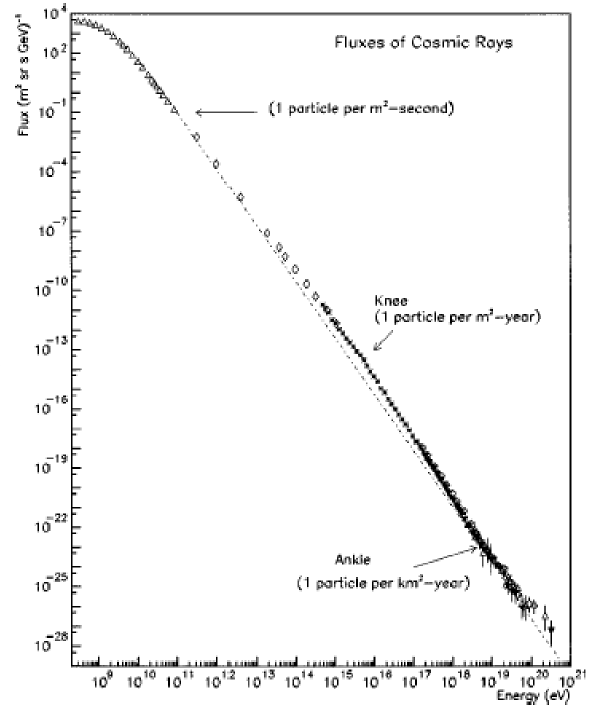

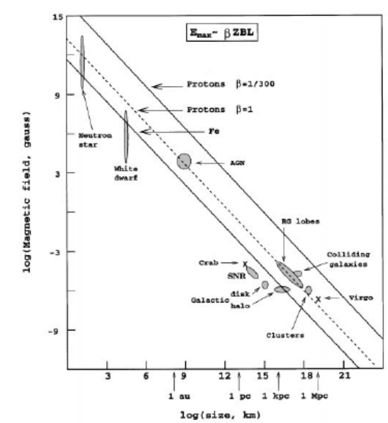

FIG. 3. Modified Hillas plot (Hillas, 1984). Size and magnetic field of possible sites of acceleration. Objects below the dashed line cannot accelerate protons to 10^{20} eV.

Roland Diehl

Dust: Condensed ISM Gas

- Condensation Temperatures Determine Dust Composition
- Macro-Particles Determine Absorption

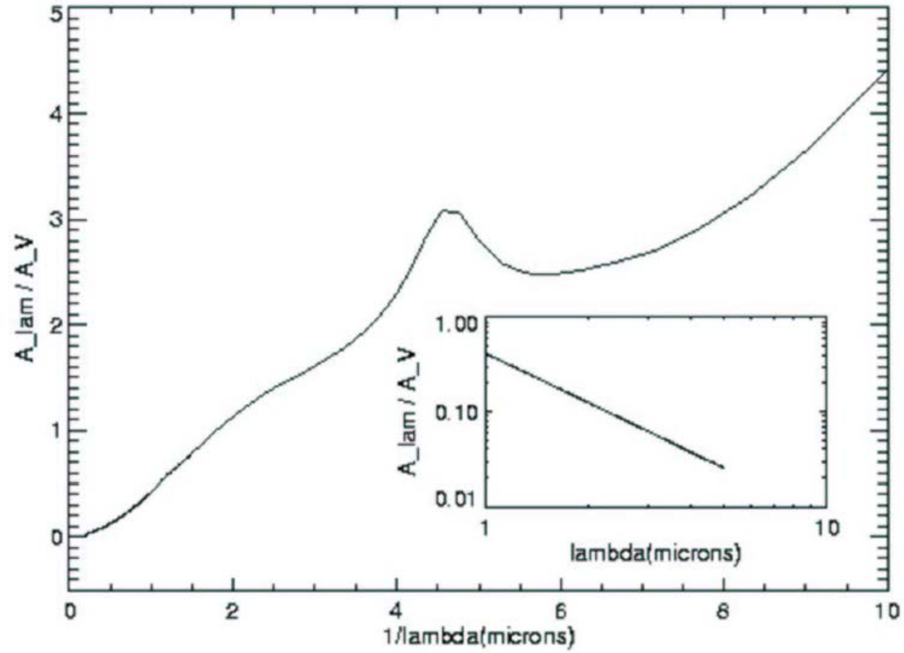

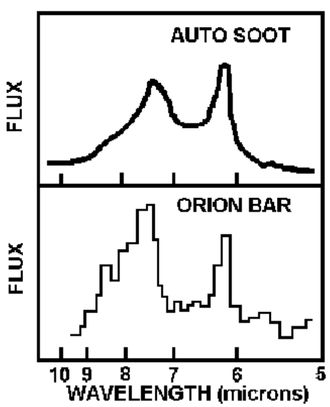

This graph shows a comparison of the infrared spectrum emitted by dust in the Orion Nebula (lower panel) and that emitted by the exhaust of a diesel truck (upper panel). Both spectra show prominent emission features at 6.2 and 7.6 micrometers that we can identify with the laboratory spectra of "Polycyclic Aromatic Hydrocarbons", or "PAHs" – known carcinogens.

Roland Diehl

ISM and High-Energy Radiation

- **Cosmic-Ray Interactions with ISM Gas**
  - ☞ Gamma-Ray Emission
    (Bremsstrahlung, Pion Decay, IC; Nuclear De-Excitation)

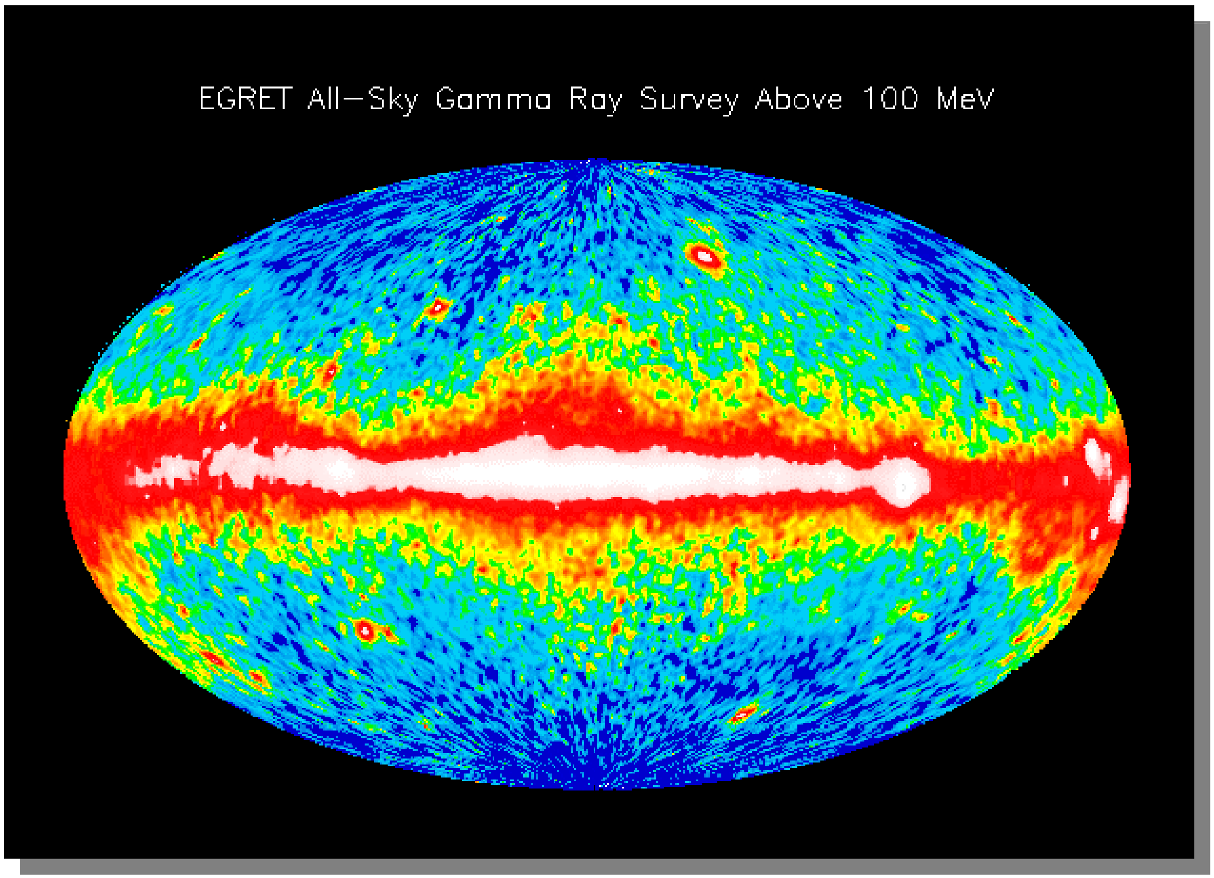

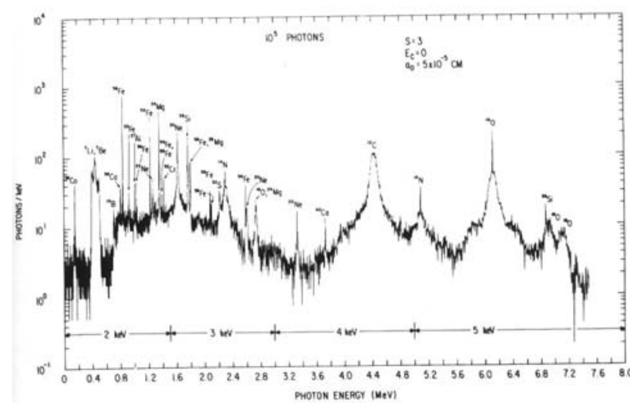

Fig. 5.12. Calculated γ-ray spectrum from energetic particles and ambient medium having solar composition. The energetic particles obey a power law spectrum in kinetic energy with spectral index s above a low-energy cutoff E_c, and the contribution from lines from interstellar grains of characteristic radius a_0 is included. From Ramaty et al. (1979 [419])

Roland Diehl

Stellar Objects: Types and Evolution

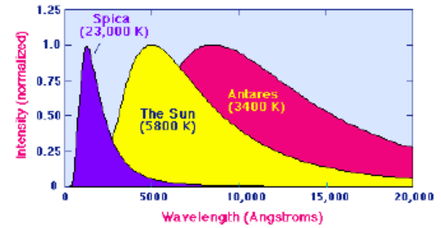

- Luminosity <-> Surface Temperature (log-log)
- Regions of Stellar States:
  - ☆ Main Sequence — H Burning Core
  - ☆ Giants — H-Exhausted Core
  - ☆ White Dwarfs — Remnant Core
- Evolution Times: $10^5 \ldots 10^{10}$y
- High-Energy Radiation:
  - ★ Coronae, Flares, Binary Interactions

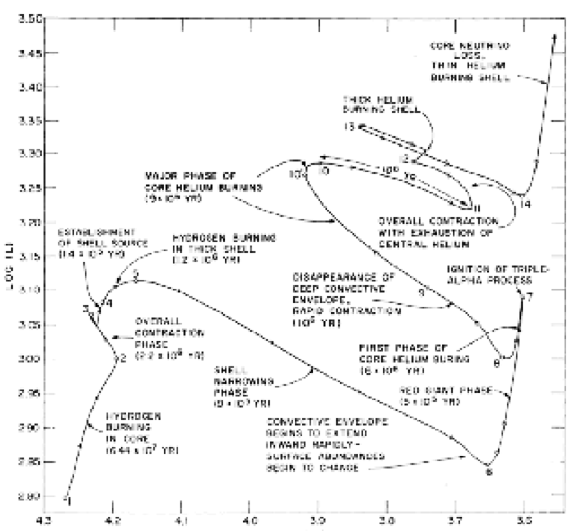

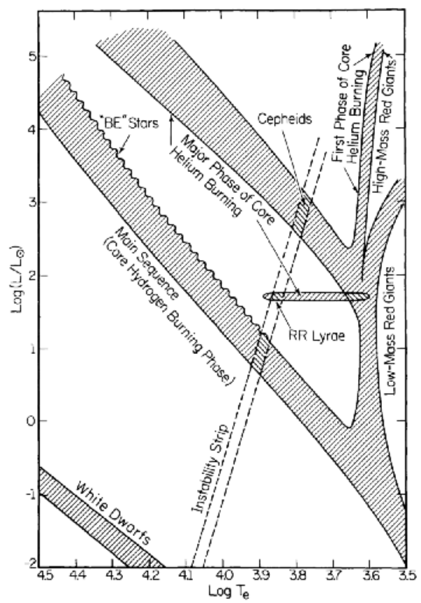

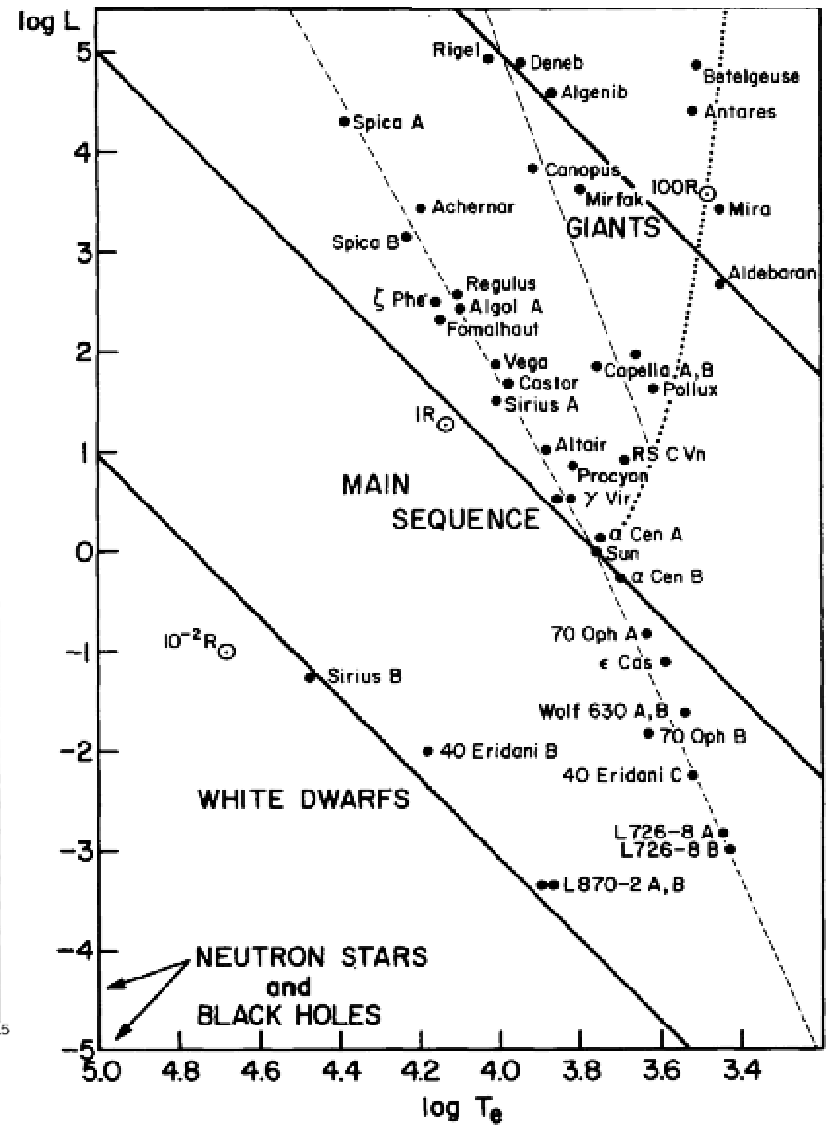

Roland Diehl

Massive Stars

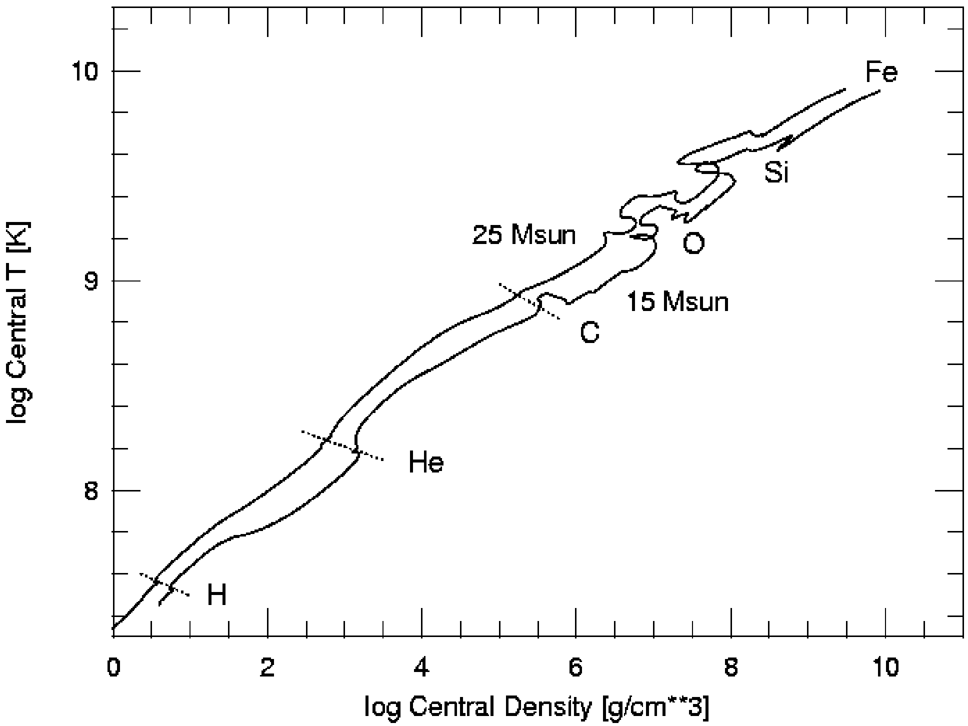

Stars := Gravitationally Confined Thermonuclear Reactors:

- Nuclear Burning of a Species (H, He, …Si)
- Gravitational Contraction when Fuel Exhausted
- …
- Degeneracy Pressure Counteracts Contraction -> White Dwarf
- For a star > 8 $M_{\odot}$: Contraction & Heating Continue until Fe Core is Made, …-> Core collapse

Roland Diehl

Nuclear Burning Stages in Stars

Advanced Nuclear Burning Stages
(e.g., 20 solar masses)

Fuel	Main Product	Secondary Products	Temp (10^9 K)	Time (yr)
H	He	^{14}N	0.02	10^7
He	C,O	^{18}O, ^{22}Ne s- process	0.2	10^6
C	Ne, Mg	Na	0.8	10^3
Ne	O, Mg	Al, P	1.5	3
O	Si, S	Cl, Ar K, Ca	2.0	0.8
Si	Fe	Ti, V, Cr Mn, Co, Ni	3.5	1 week

Roland Diehl

Stellar Evolution Tracks

- **Main Sequence Evolution**
  - ☆ H Core Burning
  - ☆ H Shell Burning
  - ☆ Red Giant Phase
  - ☆ He Core Burning
  - ☆ AGB/Planetary Nebula

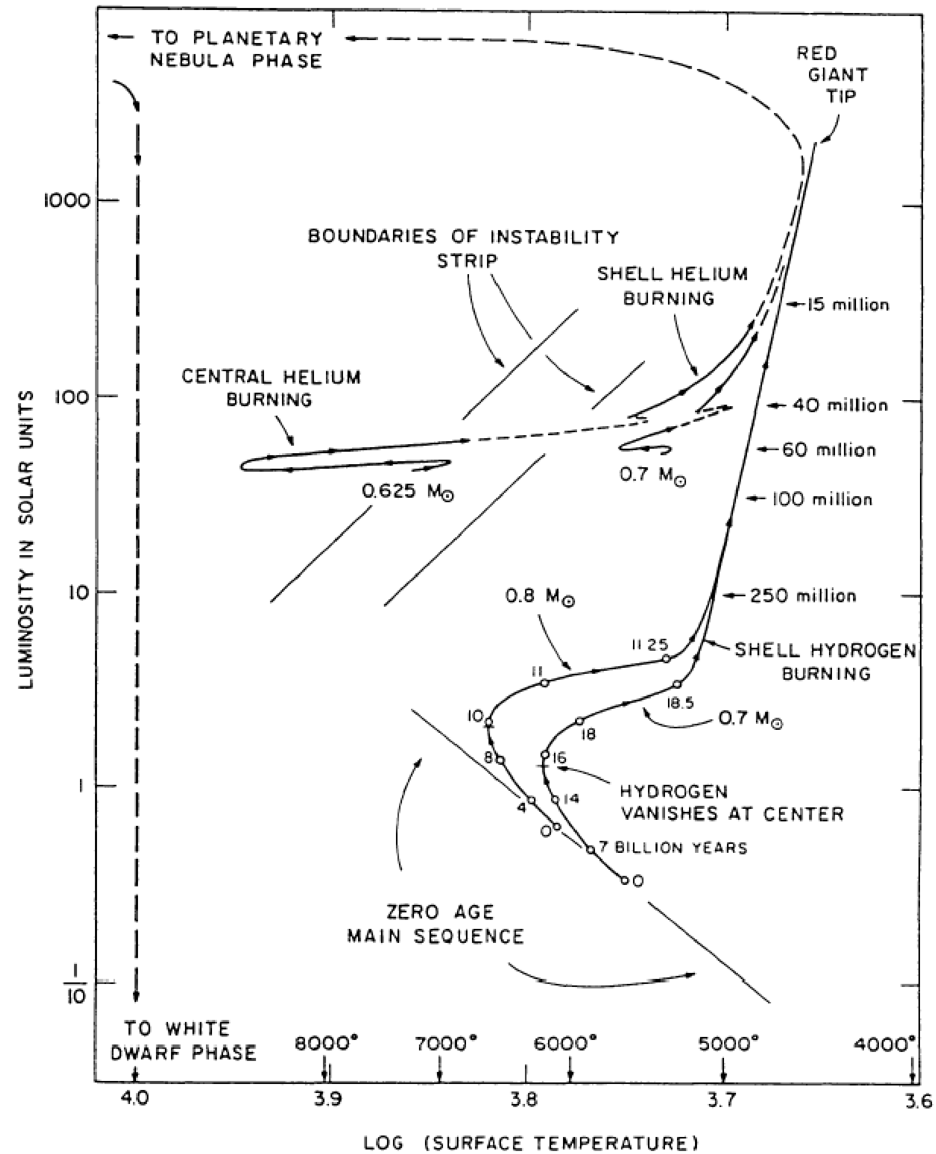

FIG. 20.—Tracks of mild Population II model stars during hydrogen and helium burning (Iben 1971*b*). Composition parameters are $Y = 0.3$ and $Z = 10^{-3}$. A number beside a circle gives the time in billions of years for a model to reach the circle from the zero-age main sequence. Times to reach the red-giant tip from points lower down on the giant branch are given in millions of years. The tracks are simplifications from the results of Iben and Rood (1970*a, b*).

Roland Diehl

Stellar Evolution

- Evolutionary Time Scale Determined by
  - ☆ Total Mass
  - ☆ Metal Content

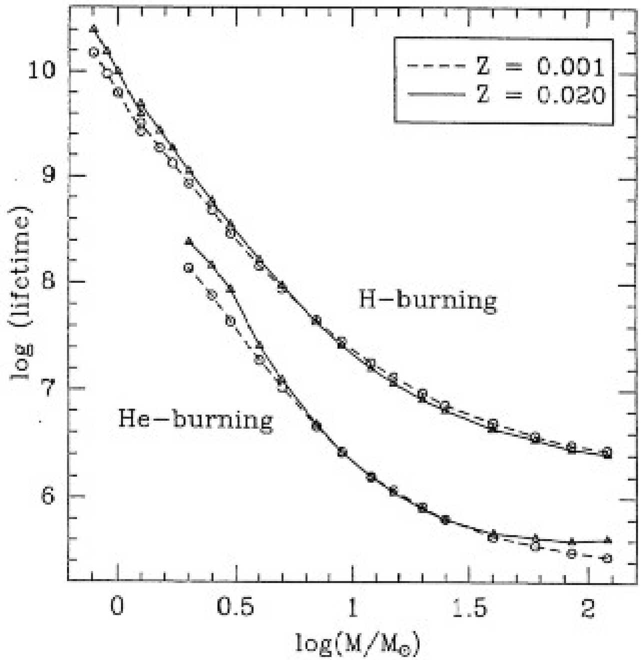

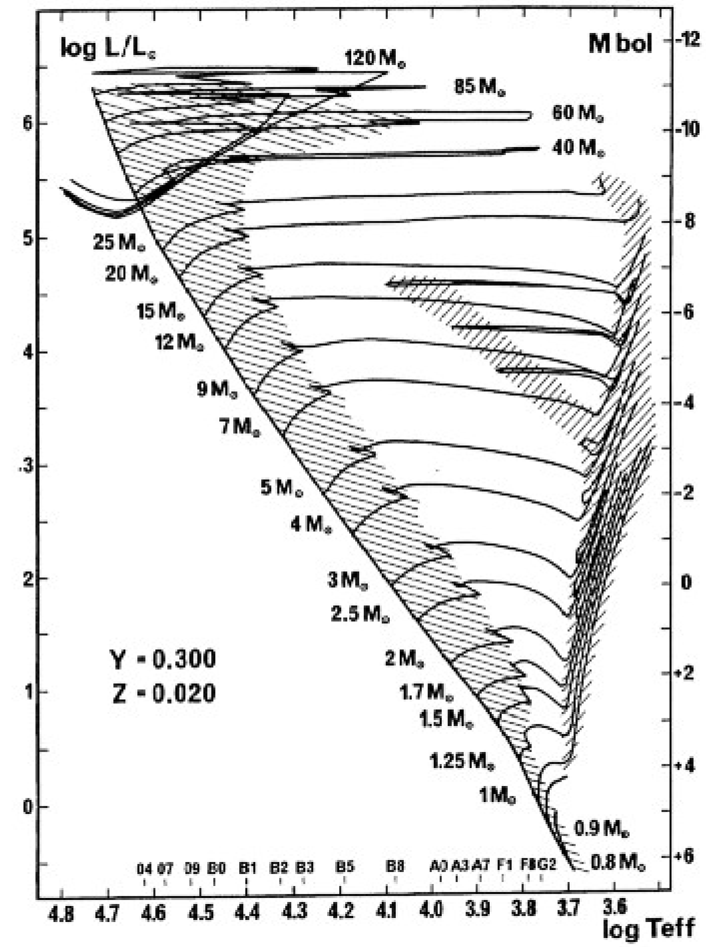

☞ Massive-Star Lifetimes ~My

☞ Low-Mass Star Lifetimes ~Gy

Stellar Structure and Evolution in Detail

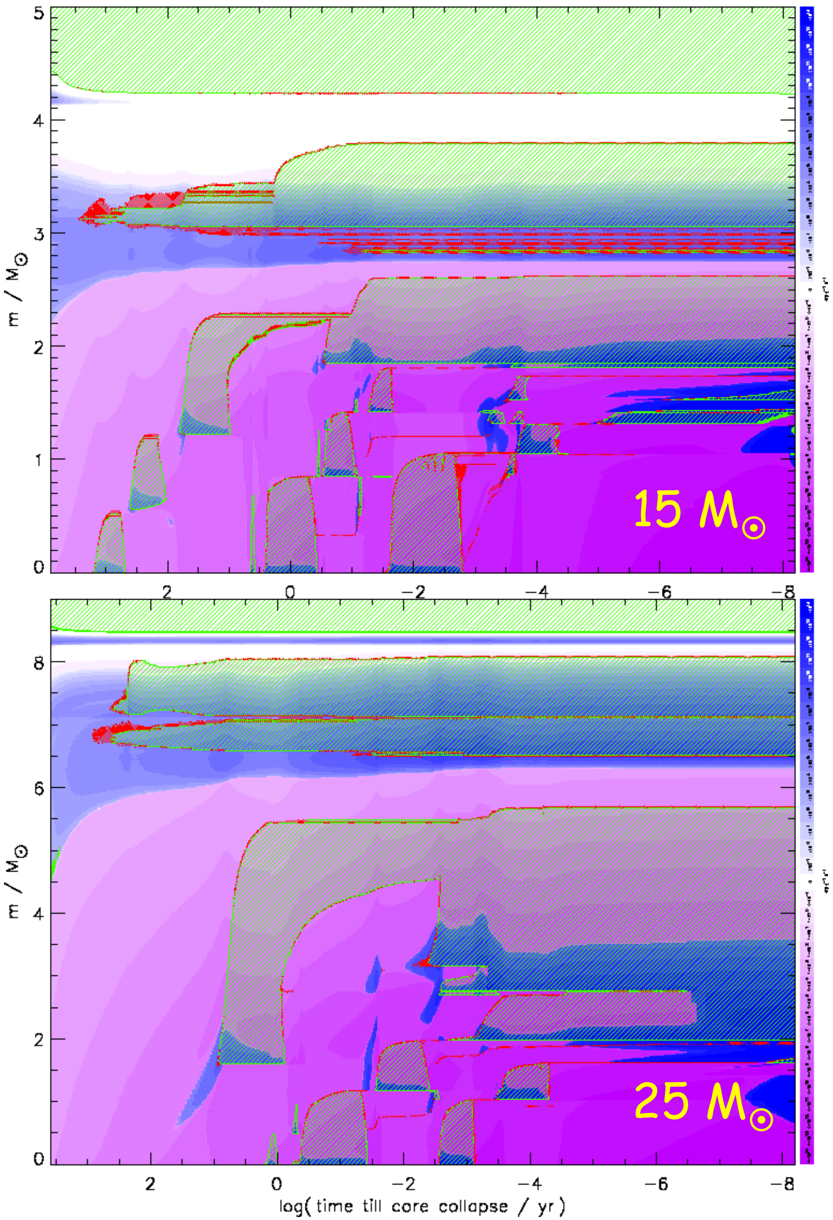

The advanced burning stages are characterized by multiple phases of core and shell burning. The nature and number of such phases varies with the mass of the star.

Each shell burning episode affects the distribution of entropy inside the helium core and the final state of the star (e.g., iron core mass) can be non-monotonic and, to some extent, chaotic.

Neutrino losses are higher and the central carbon abundance lower in stars of higher mass.

Roland Diehl

Nucleosynthesis Ejecta from Massive Stars

- Winds and SN Eject Products from Pre-SN and Explosive Nucleosynthesis
- Comparison to Standard Abundances
  - "Production Factors": 1.= SA
- Dependancies:
  - Stellar Model (e.g. Convection, Rotation)
  - Explosion Model (Piston, Bomb, Jets,…)
  - Nuclear Rates (e.g. $^{12}C(\alpha,\gamma)^{16}O$

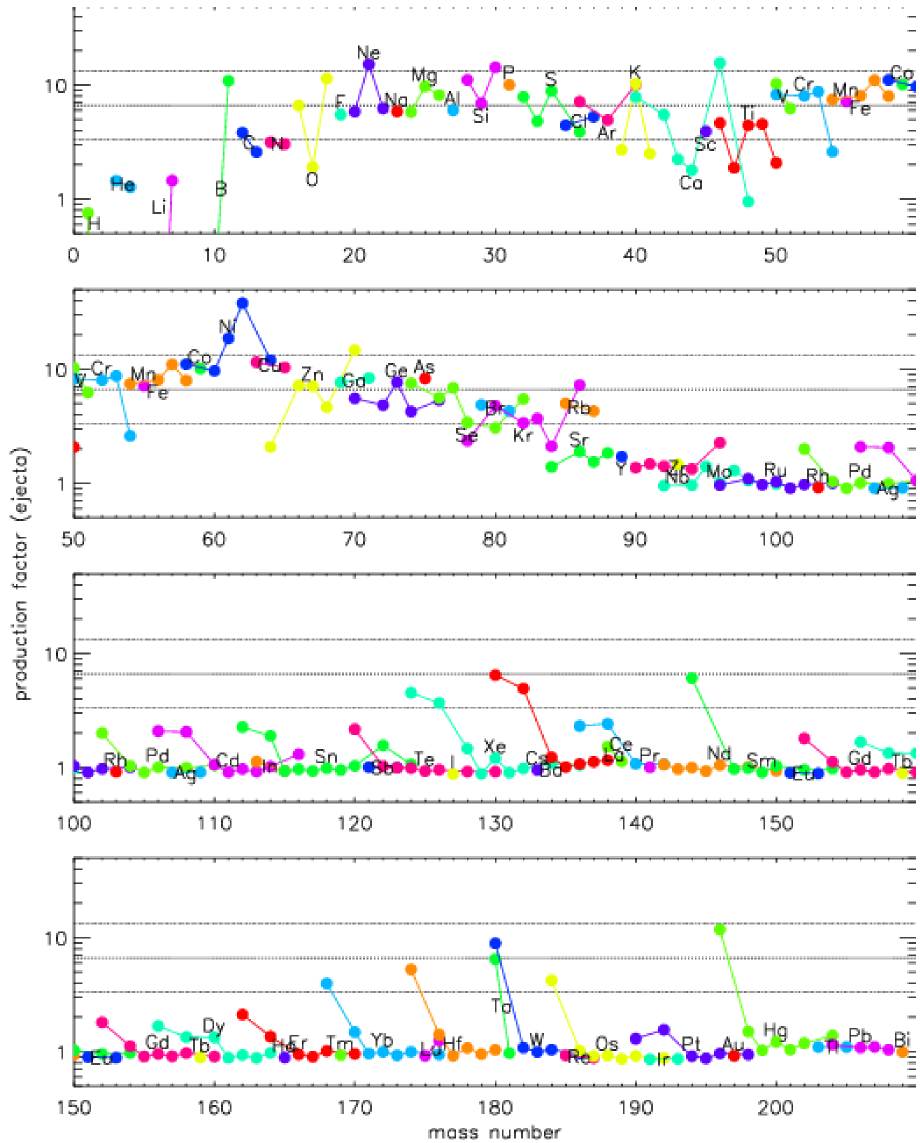

- e.g.:Rauscher, Heger, Woosley, Hoffman (2001, 2002,..)

Stellar Classification and Radiation Origin

- Spectral Classification Encodes Temperature
- Plasma Radiation Mechanism Depends on Temperature
  - ☞ Molecules and Dust
  - ☞ Neutral Atoms
  - ☞ Ionized Atoms

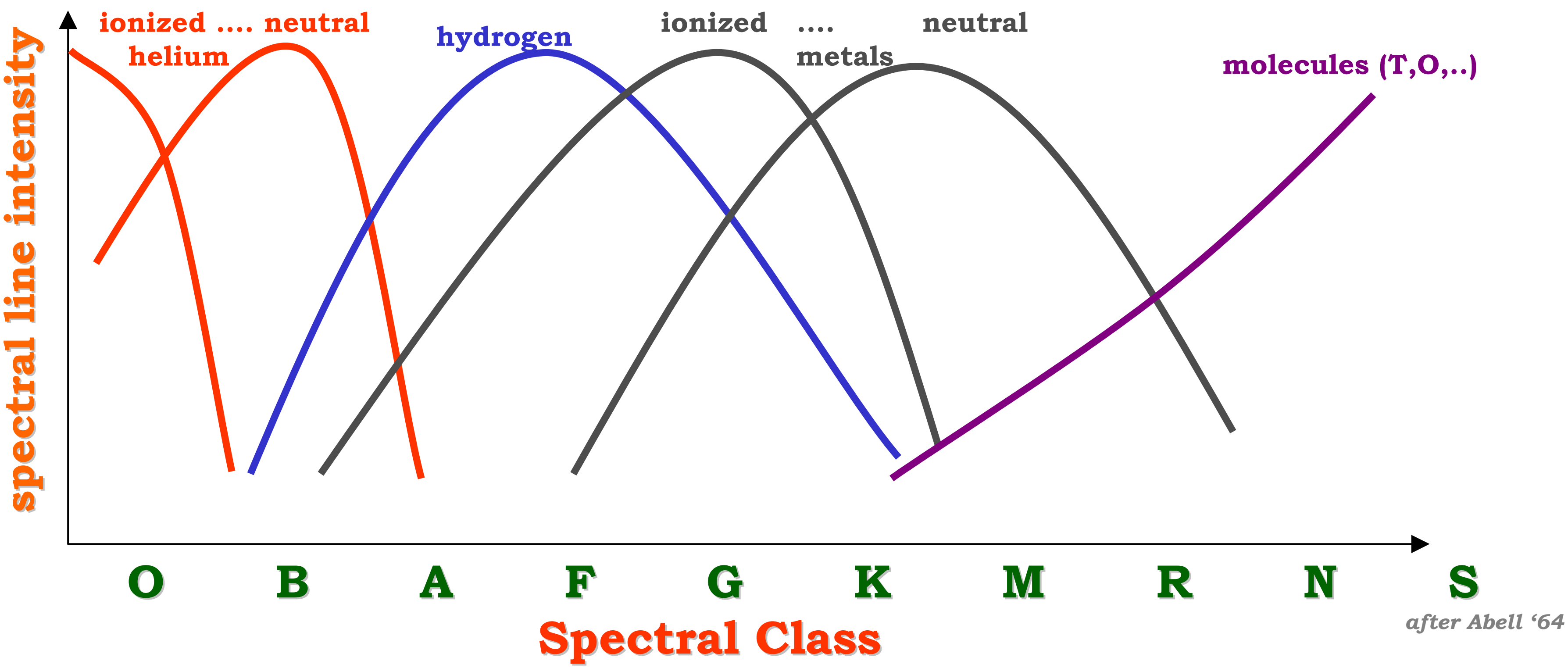

Roland Diehl

Stellar Mass Loss: Winds

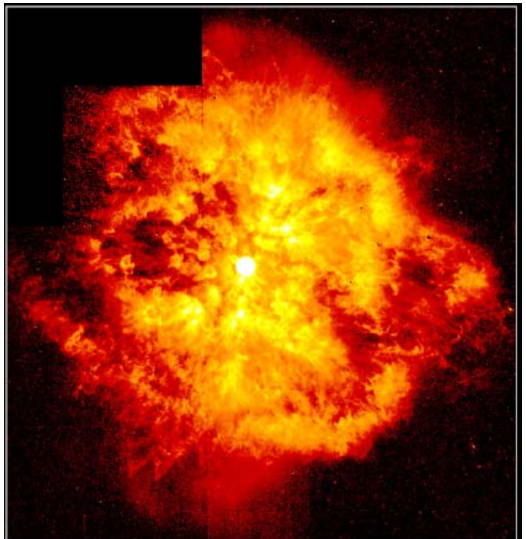

Nebula M1-67 around Star WR124 HST • WFPC2
PRC98-38 • STScI OPO • November 5, 1998
Y. Grosdidier and A. Moffat (University of Montreal) and NASA

- **Radiation Pressure Exceeds Gravity**

$$\frac{L}{4\pi R^2 c}\sigma_{Te^-} \geq \frac{GM_c}{R^2}(m_p + m_{e^-})$$

$$L_{Edd} = \frac{4\pi c G M_c m_p}{\sigma_{Te^-}} \qquad L_{Edd} = 1.3 \cdot 10^{38}\frac{M_c}{M_\odot}\left[\frac{erg}{s}\right]$$

- **Wind Characteristics of Stars**

During the post main sequence phase stars loose a major part of their mass via *winds* and *thermal pulses*:

main sequence $1M_\odot$	$\longrightarrow$	tip of AGB $0.6M_\odot$
main sequence $8M_\odot$	$\longrightarrow$	tip of AGB $0.8M_\odot$

The expelled gas is given back to the interstellar medium. At the end of the AGB-phase stars with inital masses less than 8 $M_\odot$ lost between 40% and 90% of their mass.

The winds of massive stars are driven by radiation pressure. The higher the metallicity, the more line transitions exist and can absorb photons, the higher is the mass loss in winds. The wind mass loss rates of **O,B stars** and **Wolf-Rayet stars** (evolved massive stars which already have suffered significant mass-loss) can be as high as $5 \times 10^{-5} M_\odot$/yr. The terminal wind velocities can be up to 4000km/s. M-type supergiants have mass loss rates up to $10^{-6} M_\odot$/yr but slow wind velocities up to 20km/s.

Stellar Mass Loss

- **Approximations of Mass Loss Rates:**
  - ☆ Core-H-Burning Phase
    - ☞ $\log(-dM/dt) = 1.67 \log(L) - 1.55 \log(T_{eff}) - 8.29$ **(only < LBV Phase)**
  - ☆ RSG Phase
    - ☞ $\log(-dM/dt) = 0.8 \log(L) - 8.7$
  - ☆ WR Phase
    - ☞ $\log(-dM/dt) = \log(L) - 10$
- **Dependencies**
  - ☆ Metallicity Dependence
    - ☞ $dM/dt \sim Z^{\xi}$ with $0.5 < \xi < 1$
  - ☆ Stellar-Mass Dependence (T)

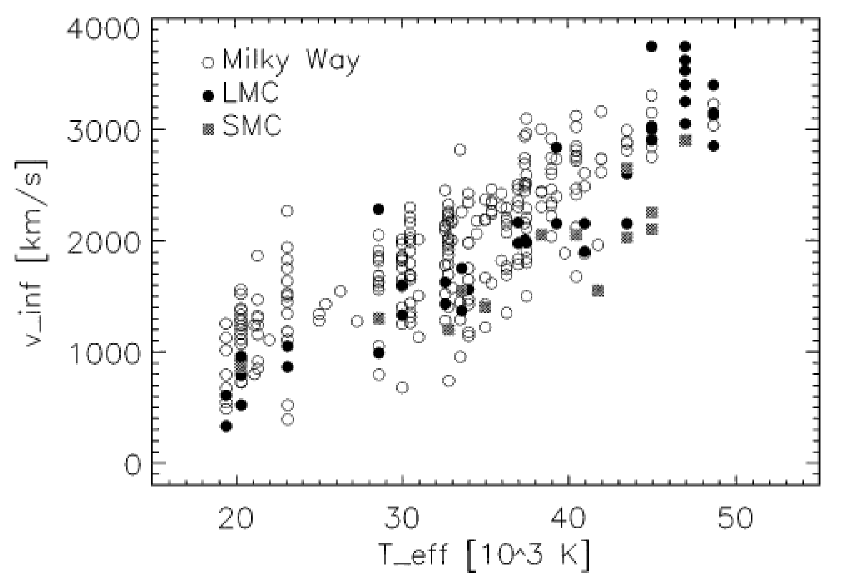

Mass-Losing Stars: Planetary Nebulae

- ☆ Ionization of CSM for T_{star} > 25000K
- ☆ Recombination Radiation -> Colorful Emission
  - ☞ Dominated by OIII forbidden lines (E2; 495.9 and 500.7 nm)

- ☆ **PN Characteristics**
  - ☞ Density ~x 10^{-3} cm^{-3} (from forbidden lines)
  - ☞ Radii ~0.3 pc
  - ☞ v_{exp}~20-30 km s^{-1}
  - ☞ Lifetime ~10^4 y

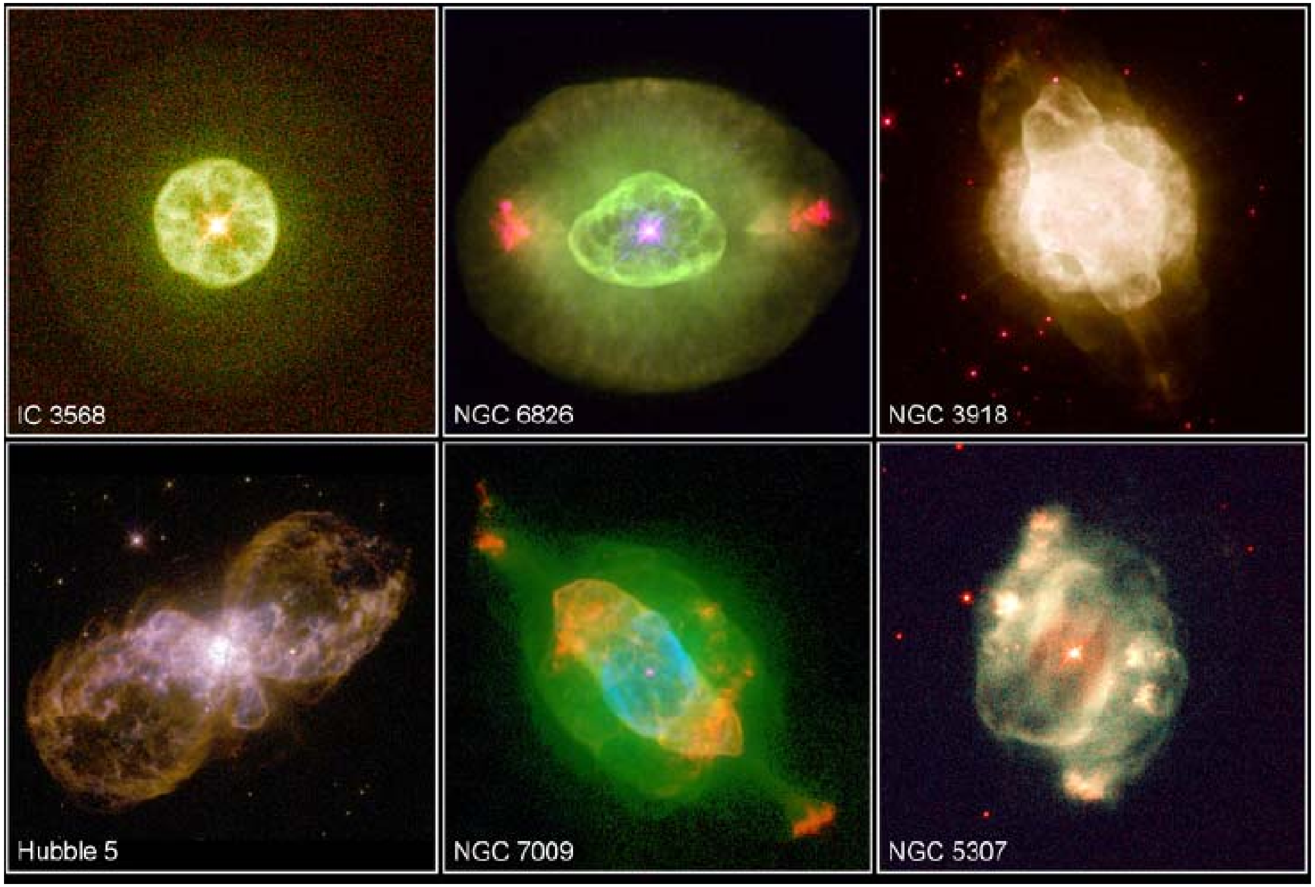

Mass-Losing Stars: WR Stars, LBV's

- Wolf Rayet Stars:
  - ☆ Strong Mass Loss Reveals Inner Structure
    - ☞ He, C, N, O -> W-Subcategories
  - ☆ Dense and Strong Wind
    - ☞ Mass Loss ~10^{-4} M_o y^{-1} over >10^5y -> many M_o
    - ☞ Wind Velocities ~100...1000 km s^{-1}
    - ☞ Optically-Thick Winds (-> Photosphere in Wind; Broad Emission-Line Spectrum)

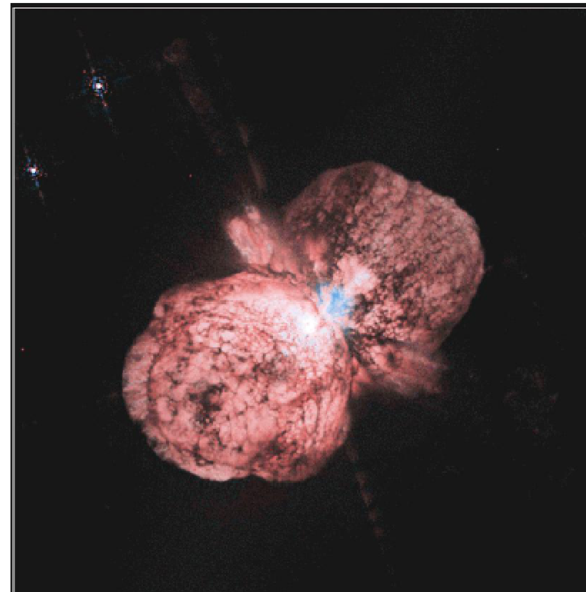

Eta Carinae
Hubble Space Telescope • WFPC2

Roland Diehl

Binary Stars: Mass Transfer and Evolution

- **Multiplicity**
  - ☆ ~50% of Stars in Binaries
- **Evolution**
  - ☆ For Large Separation: ~like Single Stars
  - ☆ Close Binaries: Mutual Interactions Affect Evolution
    - ☞ Tidal Forces
    - ☞ Mass Transfer

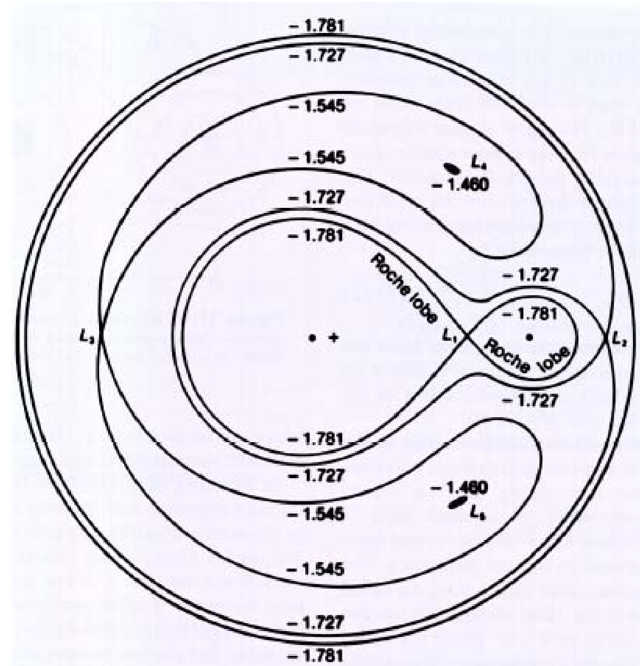

The mass transfer between binaries is determined by the Roche potential:

$$\Phi = -\frac{GM_1}{r_1} - \frac{GM_2}{r_2} - \frac{1}{2}\omega^2 s^2$$

where ω is the rotation period and s is the distance to the rotation axis.

Within the Roche-surface matter is bound to M_1 or M_2, outside of it, it is bound to both objects. The **inner Lagrange-point** L_1 is force free. At L_1 matter can easily move from one star to the other.

Roland Diehl

Binary System Evolution

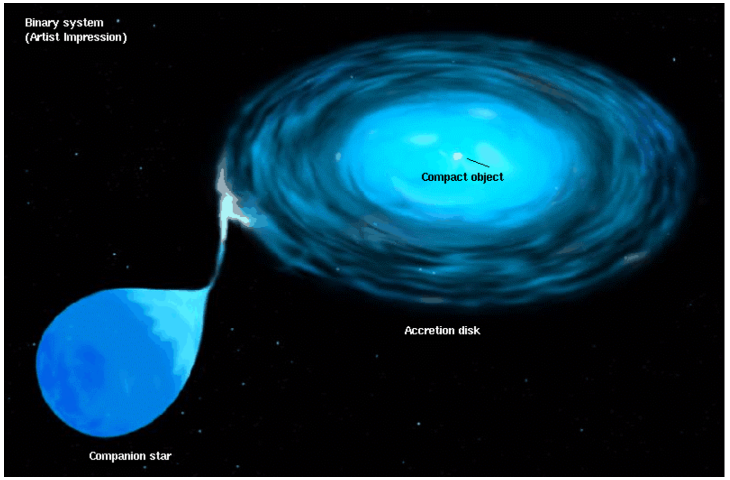

- **Characteristics**
  - ☆ Mass of Components
    - ☞ High-Mass Binaries
    - ☞ Low-Mass Binaries
  - ☆ Orbits and Mass Transfer
    - ☞ Interacting / Quiet Phases for Elliptical Binaries (e.g. WR140)
      - Wind Interactions, CR & Dust Formation
    - ☞ Accreting Binaries
      - Accretion Rate / Disk Instabilities: Cataclysmic Variables , QPO's
      - Transient Events from Accreted Layer: Novae, Type I X-ray Bursts, Thermonuclear Supernovae
    - ☞ Metal-Enriched Envelope
      - Unusual Radiation Characteristics and Wind Phases
      - Evolution Unlike Single Star

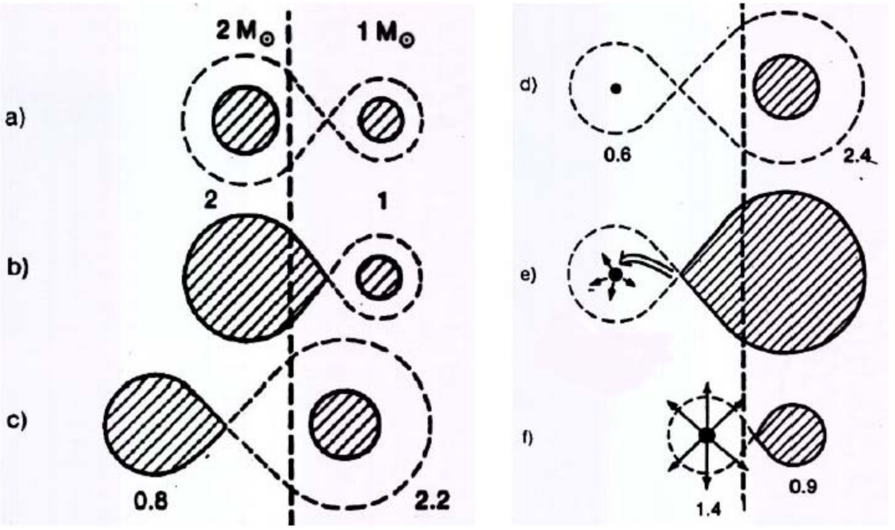

Binary Evolution: Loss of Angular Momentum

- Binary System Shrinking from
  - ☆ Magnetic & Tidal Torques
  - ☆ Gravitational Waves
  - ☆ Accretion Disk Radiation

☞ Possibility of Merging

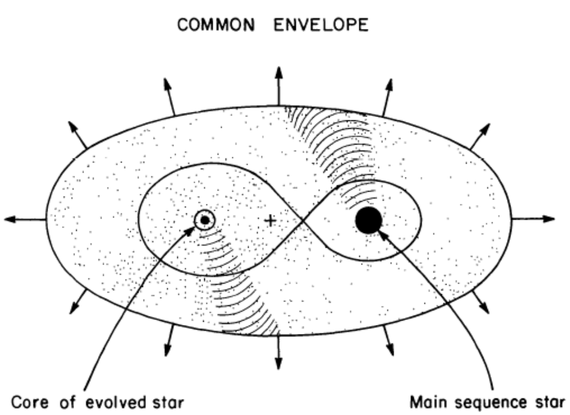

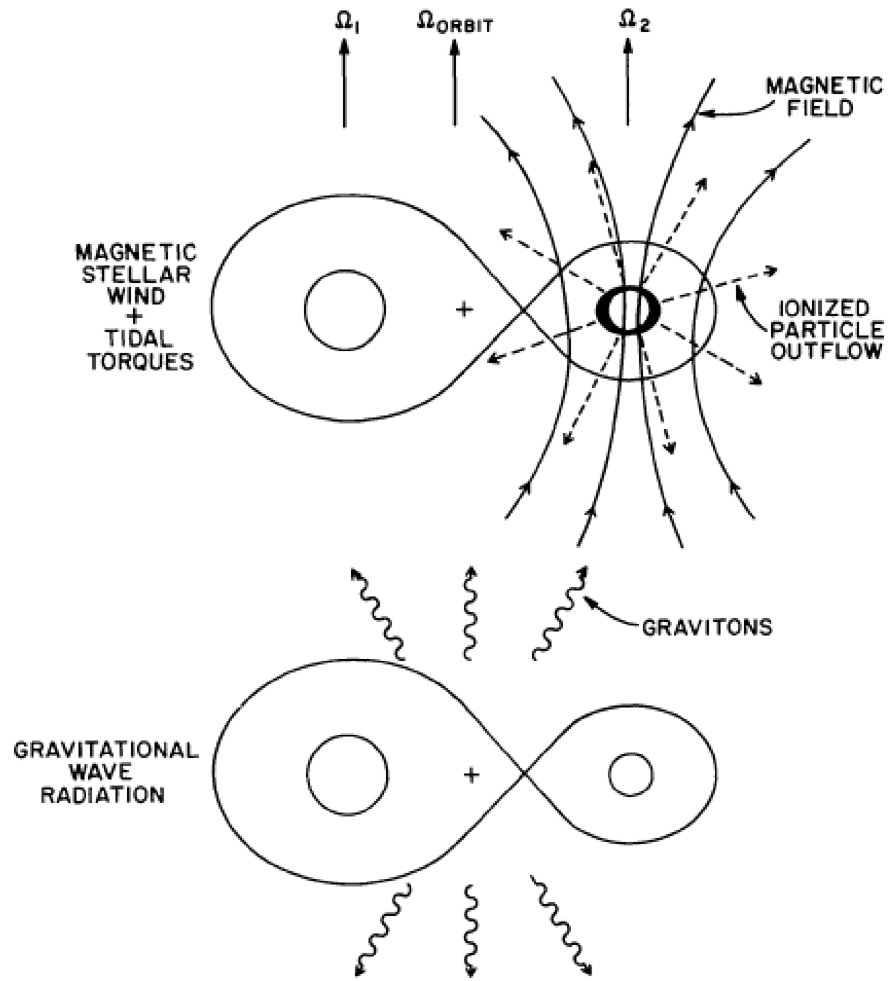

FIG. 12.—Schematic describing two modes of angular momentum loss: due to a magnetic stellar wind and tidal torques (MSW), and due to gravitational wave radiation (GWR).

Results of (Binary) Evolution: White Dwarfs

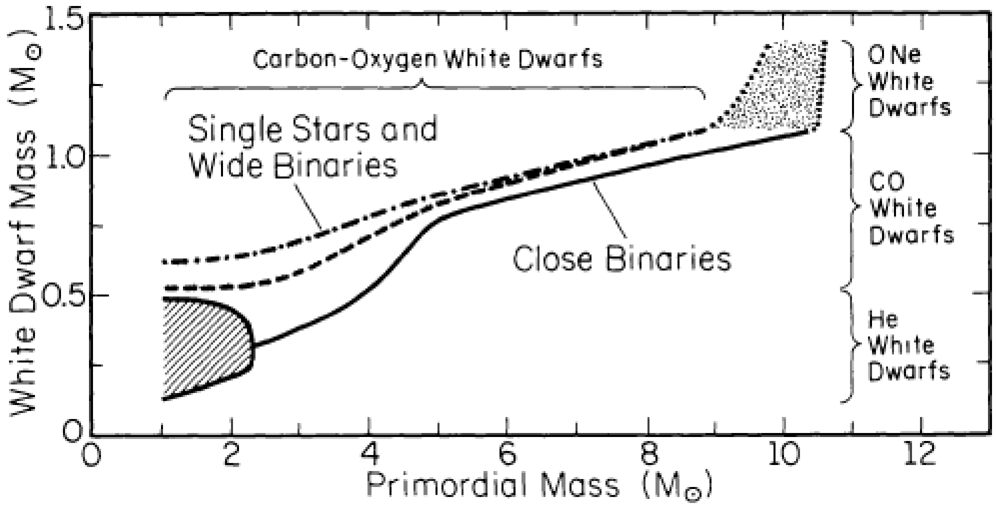

- **Composition and Size of WD Depend on**
  - ☞ Companion's Mass Transfer
  - ☞ Stellar Mass and Metallicity
- **WD Mass Spectrum**
  - ☞ Peak at ~0.5-0.6 $M_\odot$

Massive-Star Binaries

- **Binary Evolution:**
  - Mass Transfer Between Close O/B Stars
  - Formation of Rejuvenated O Star and He Star
  - Supernova of He Star
  - Formation of NS Binary
  - Formation of WR / NS Binary or Thorne-Zytkov Object
  - Supernova of WR Star

- **Binary Fraction ~50%**

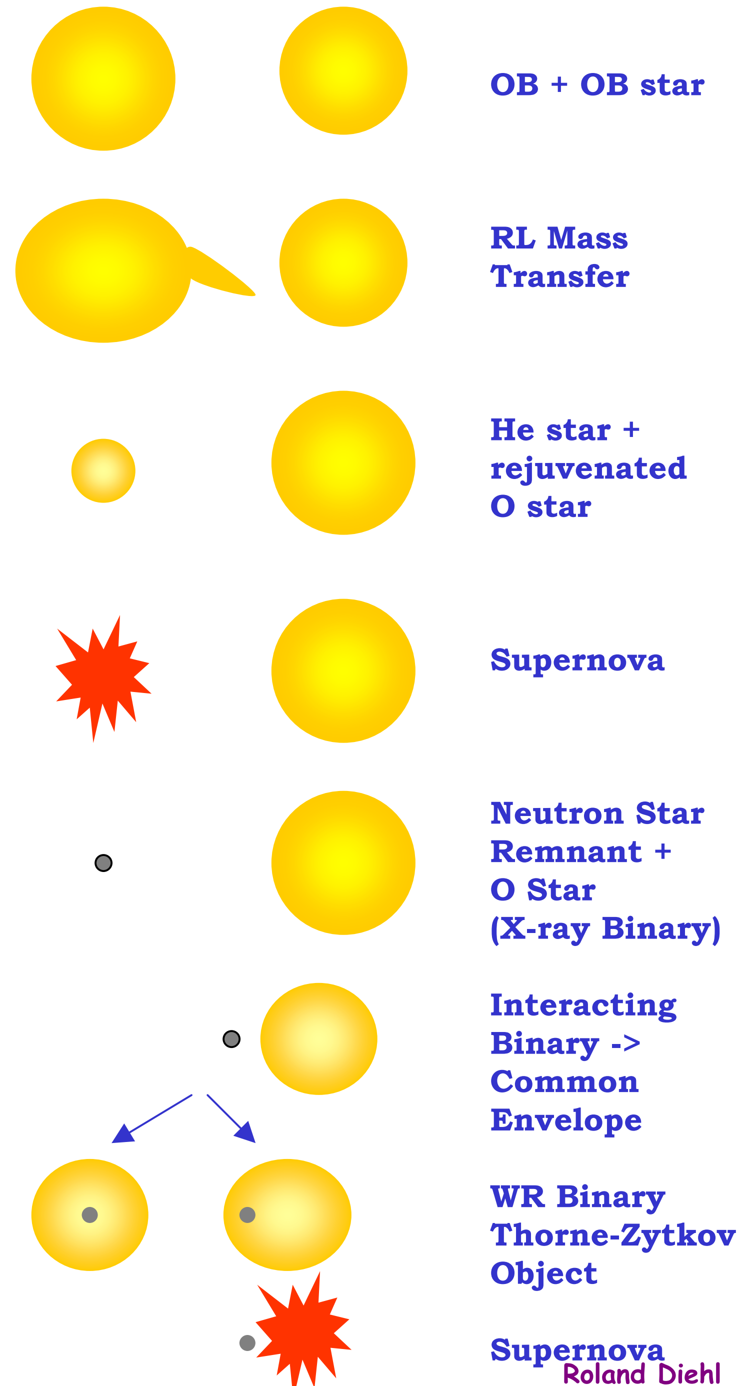

Roland Diehl

Accretion onto Compact Objects

- ☆ Angular Momentum of Matter Flow from Companion -> Accretion Disk
- ☆ Accretion Flow Dynamics -> Luminosity / Spectral "States", Instabilities
- ☆ Radiation Sources:
  - Accretion Disk
  - Corona
  - Compact-Star Surface

☞ Scattering, Absorption

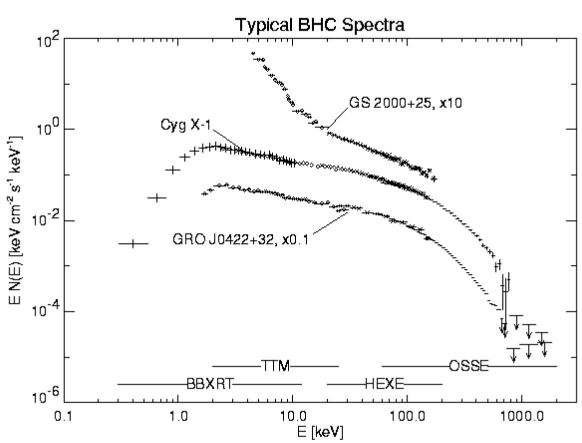

(Cyg X-1: Wilms et al., 1996, ; GRO J0422+32, GS2000+25: Sunyaev et al., 1993, Kroeger [priv. comm.])

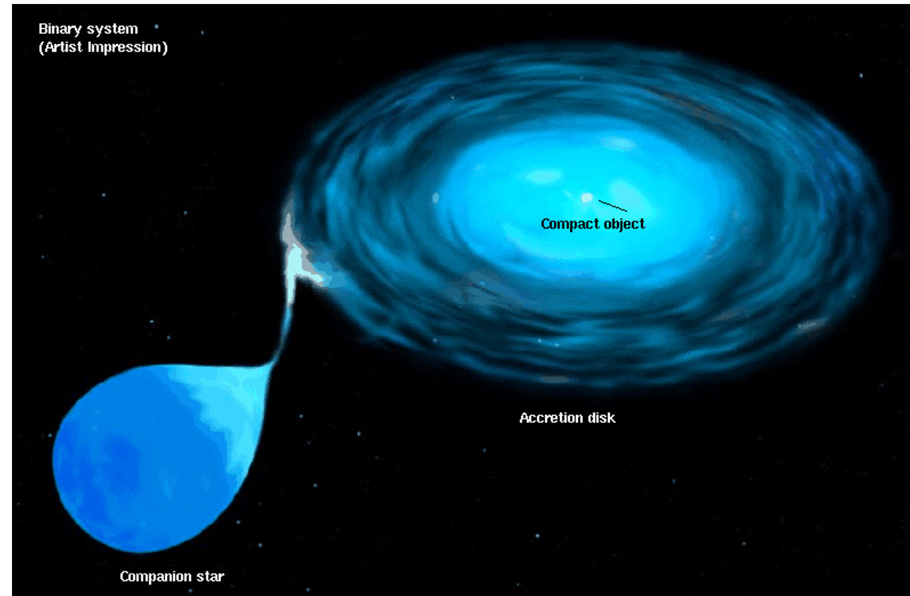

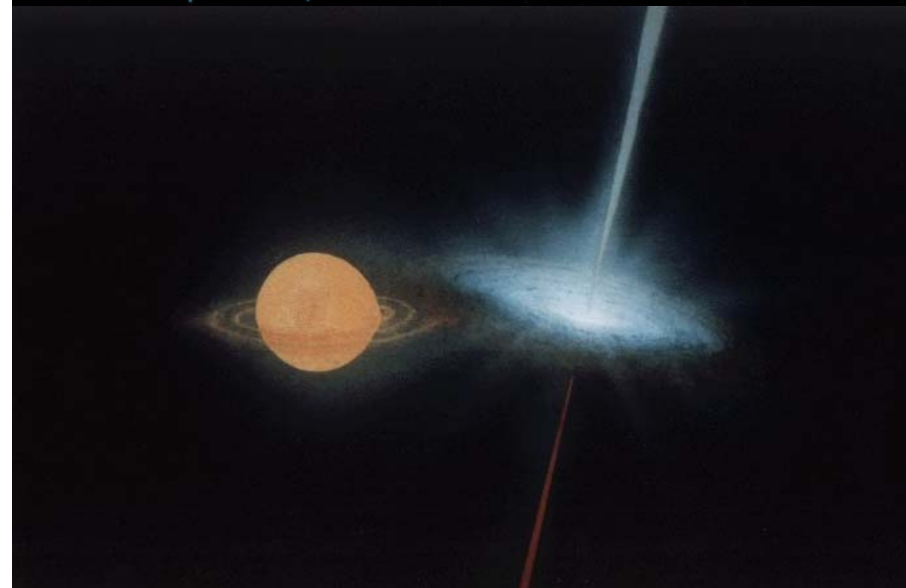

Roland Diehl

Plasma Jets from Accreting Compact Stars

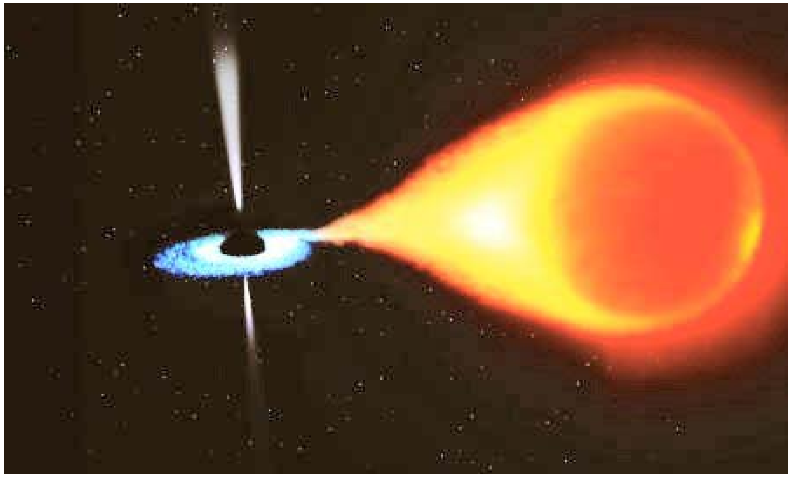

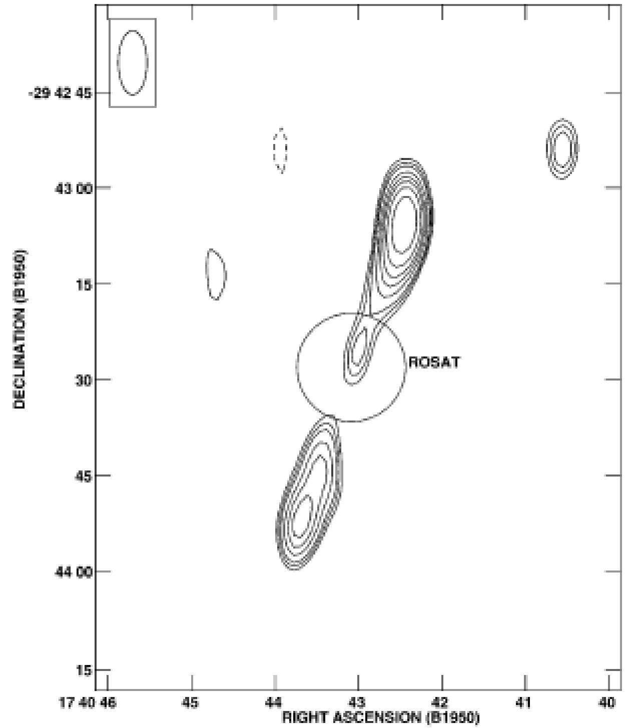

Figure 1 Contour map of the 6-cm emission from the radio counterpart of 1E1740.7-2942, as observed with the Very Large Array (Mirabel et al 1992; Rodriguez & Mirabel 1999c). The error circle of the ROSAT position (Heindl et al 1995), that includes the core source, is also shown. At a distance of 8 kpc the length of the jet structure would be ~5 pc. The half power contour of the beam is shown in the top left corner. Contours are −4, 4, 5, 6, 8, 10, 12, 15, and 20 times 28 μJy beam^{-1}.

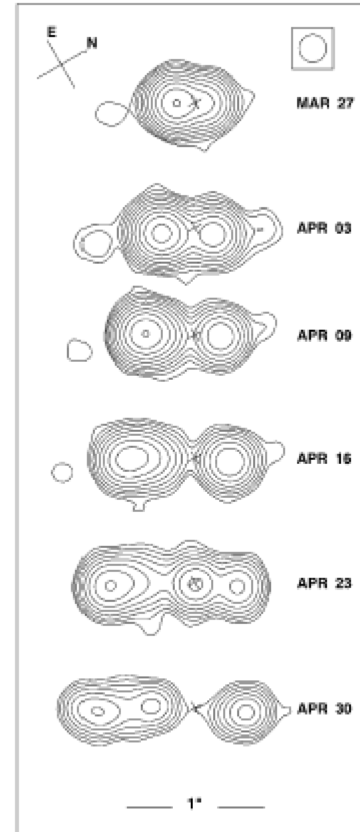

- "Micro-Quasars" from Jets of Accreting Stellar-Mass Sized Compact Objects
- X-Ray and Radio/γ Emission from Hot Plasma & Relativistic Particles
- "Superluminal" Plasma Blobs Traced in Radio Emission

Supernova Ia Models

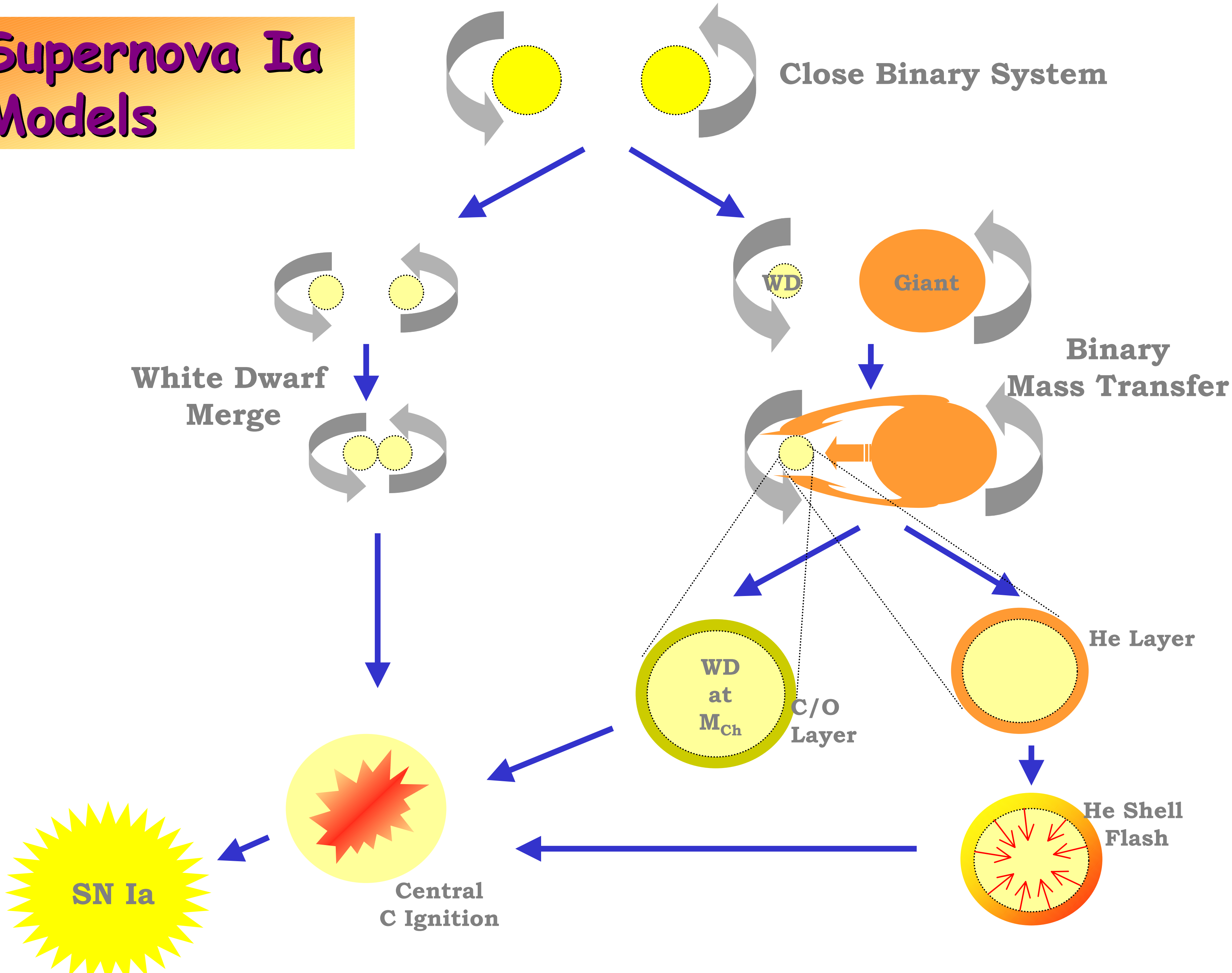

Roland Diehl

Neutron Star Mass Loss: Pulsar Winds

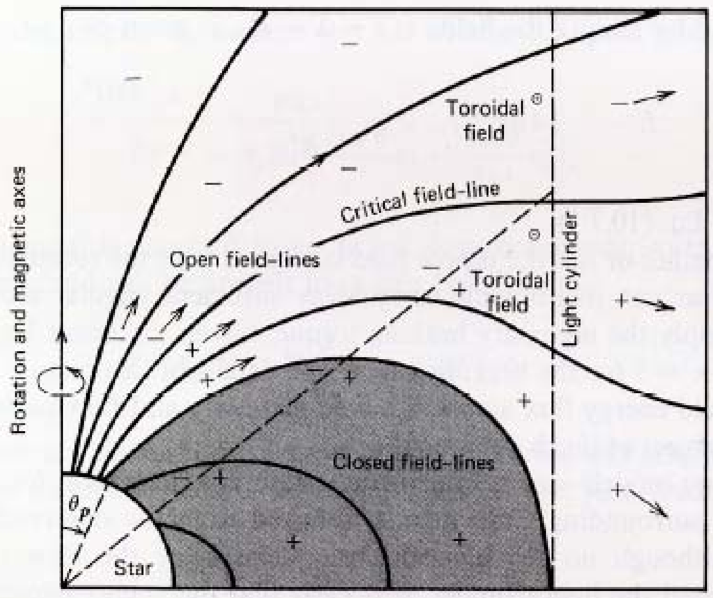

Figure 10.6 Sketch of the Goldreich–Julian (1969) model of the magnetosphere of a pulsar with parallel magnetic and rotation axes. Particles that are attached to closed magnetic-field lines corotate with the star and form the corotating magnetosphere. The magnetic-field lines that pass through the light cylinder (where the velocity of corotation equals the velocity of light) are open and are deflected back to form a toroidal field component. Charged particles stream out along these lines. The critical field line is at the same electric potential as the exterior interstellar medium. This line divides regions of positive and negative current flow from the star and the plus and minus signs indicate the charge of particular regions of space. The diagonal *dashed* line is the locus of $B_z = 0$, where the space charge changes sign. The angle subtended by the polar cap region containing open field lines is θ_p. [From *Pulsars* by Richard N. Manchester and Joseph H. Taylor. W. H. Freeman and Company. Copyright © 1977.]

- Rotation of Strongly-Magnetized Star:
  - ☆ Open Magnetic Field Lines ("Light Cyclinder")
  - ☆ Particle Acceleration in "Gaps"
    - Inner Gap
    - Outer Gap

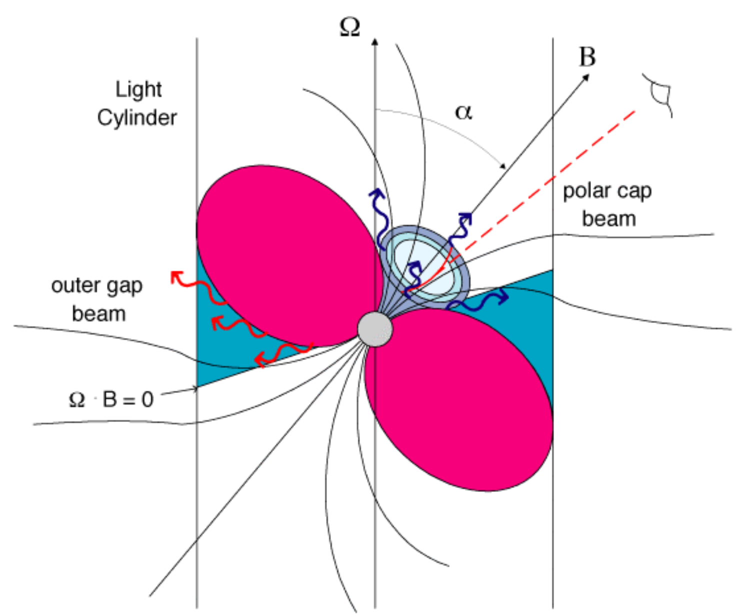

Supernovae

- Explosion of a Star
- Nuclear Energy Release
  - ☆ Radioactive By-Products of Explosive Nucleosynthesis
  - ☆ Progressive Transparency of Exploding Star
  - ☆ Thermonuclear Supernovae (Type Ia)
  - ☆ Gravitational Collapse Supernovae (Types II, Ib/c)

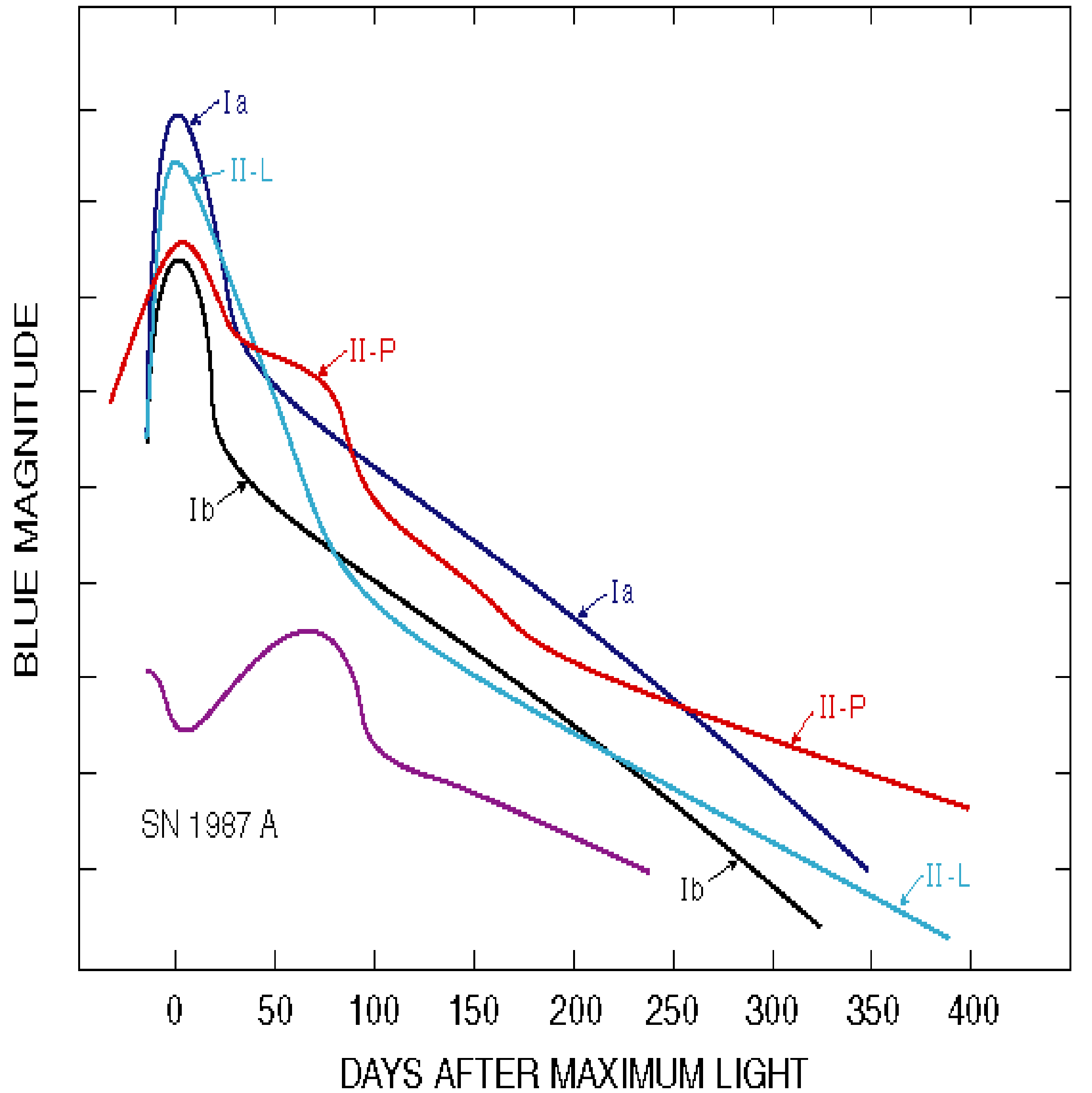

Roland Diehl

Matter Recycling by Supernovae

- E(explosion) ~ 10^{51} erg (~BE(Fe-Core))
  -> Ejection of Part of Star (Envelope)
- Independent of SN Brightness (~M_{56Ni})
- Major Mass Loss Occurs Before the SN (M_{core}~ 4-6 $M_\odot$)

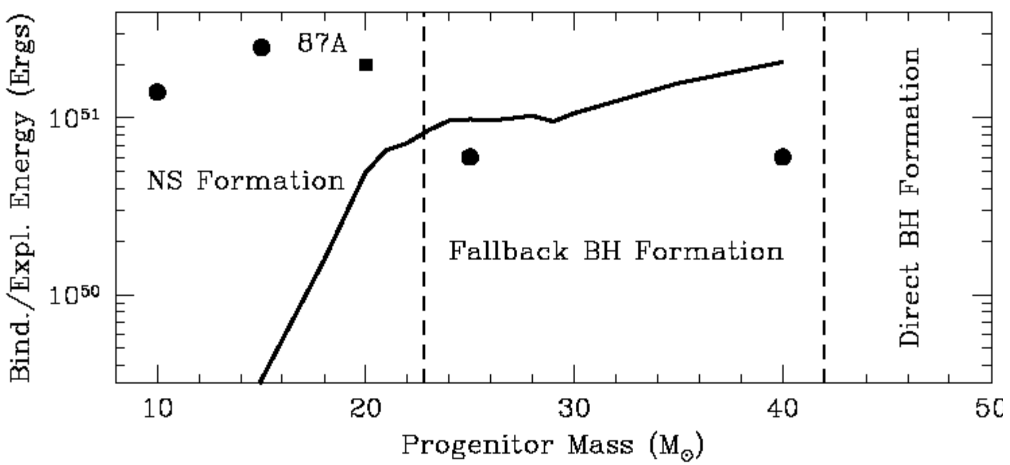

Figure 3. Binding energy/explosion energy *vs.* progenitor mass assuming no mass loss. The solid line is the binding energy of all but the inner 3 $M_\odot$ of the stellar core. If the explosion energy is not at least this powerful, the star will collapse to a black hole. The four circular dots denote the explosion energies from core-collapse simulations and the square is the predicted explosion energy observed from SN 1987A.

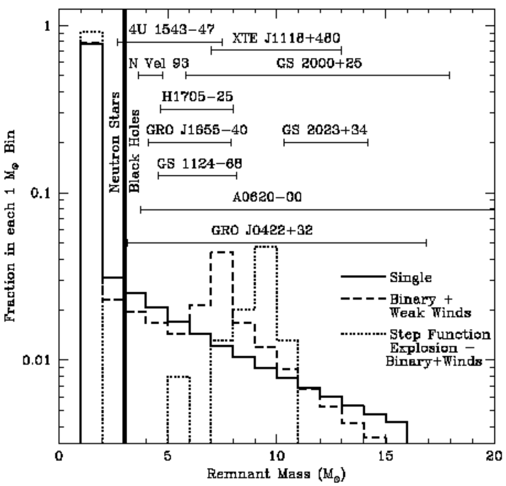

Figure 4. Mass distribution of black holes and neutron stars using the best fit to the Fryer (1999) explosion energies for single stars (solid line) and binary stars with weak winds (dashed line) along with the step-function explosion energy for binary stars and weak winds (dotted lines). The data of observed systems with their error bars are plotted as well.

Mixing of Galactic Gas

- Mixing Time Scale Driven by
    - ☞Large-Scale Motion and Turbulence (Galactic Rotation,…)
    - ☞Supernova Input of Localized Turbulence

☆ "Instantaneous Recycling" is only Crude Approximation

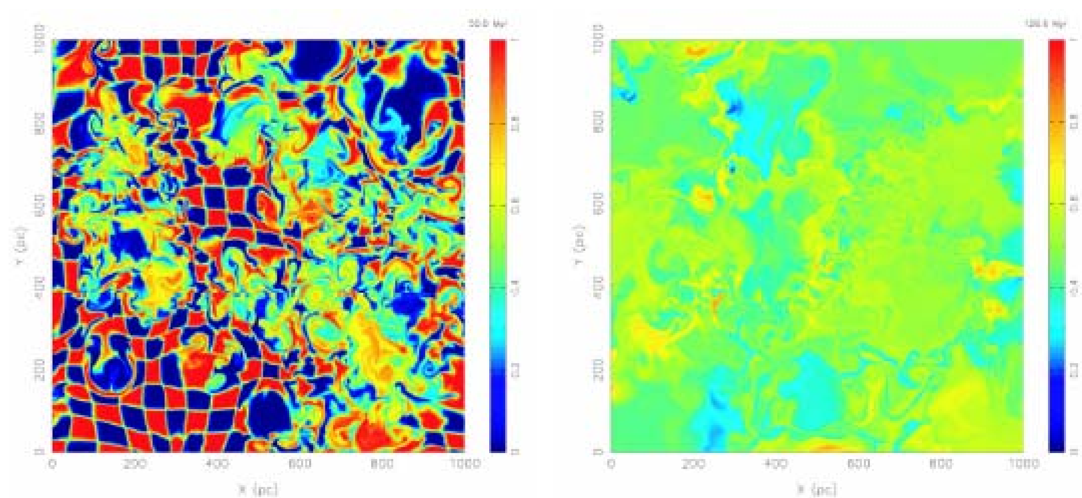

FIG. 4.—Distribution of inhomogeneities with length scale $l = 50$ pc at times 50 and 126.6 Myr of evolution for the Galactic SN rate. The resolution of these images is 1.25 pc.

Roland Diehl

Cosmic Evolution: Data

- Chemical Species
  - ☆ Metallicity
  - ☆ Primary versus Secondary Isotopes
  - ☆ Galactocentric Gradients
  - ☆ Galaxy Type Characteristics
- Star Formation
  - ☆ Supernova Rates
  - ☆ Dust Emission
  - ☆ Ionized-Gas Emission (Hα)
  - ☆ Blue-Light Emission
- Link: "Chemical Evolution"

Chemical Evolution

- Basic Considerations
  - ☆ Gas Consumed by Star Formation, Provided by Winds and SN
  - ☆ Stellar Properties Determine Wind and SN Properties
  - ☆ Gas Properties Determine Star Formation Rate
  - ☆ Instantaneous Recycling Assumed
  - ☆ Extragalactic Flows (Infall, Wind Loss) Added

Galactic Halos and Intergalactic Gas

- Galactic Winds & Fountains Eject Gas into Intergalactic Space
- Inefficient Cooling (hot plasma, low density), Unknown Heating Sources (magnetic fields, CRs, turbulence)
- Recording IGM Gravitational Potential and Chemical History

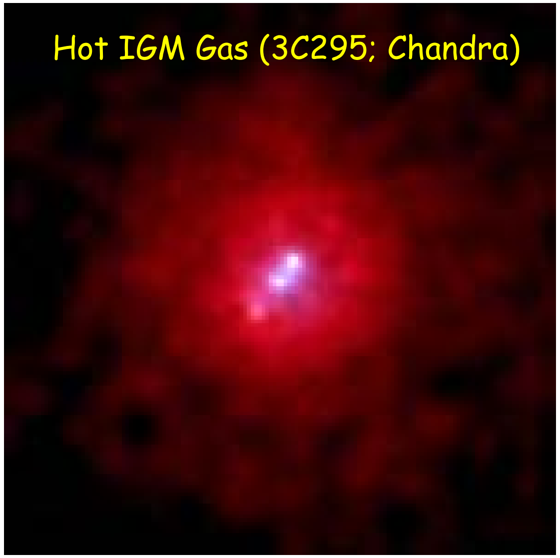

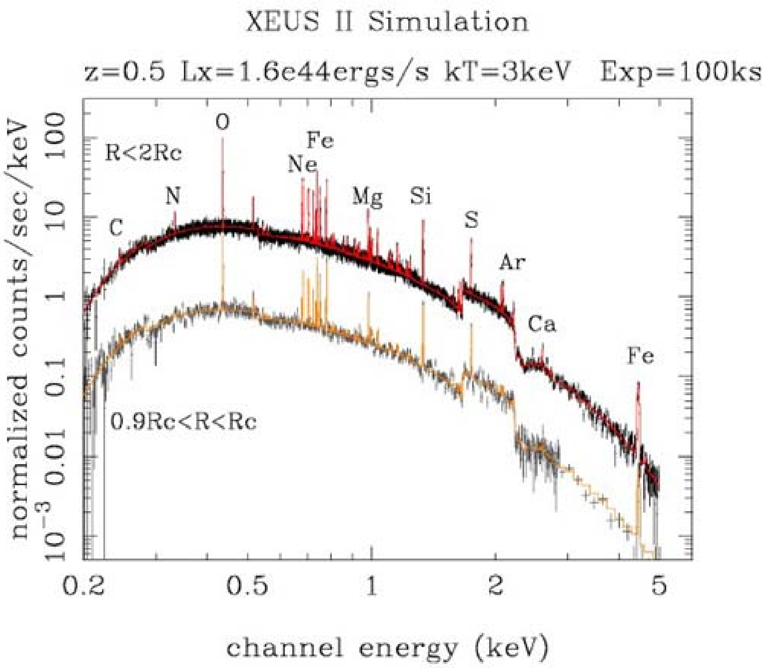

Massive-Star / ISM Interactions and γ-Rays

- Massive Stars Often Form in Groups
- Massive-Star Winds and SNae Determine the ISM Morphology
- Massive-Stars' Metal-Enrichment of ISM Produces Diffuse Radioactivities
- Evolution Time Scale of Stellar Groups: ~ 10-100 Myr
- Evolution Time Scale of Massive Stars: ~0.1-10 Myr
- Radioactive Decay Time of ^{26}Al: 1 Myr
- Cosmic-Ray 'Propagation Age' ~10 Myr
- Evolution of Radiation Phenomena, Occultation Issues
- γ-Ray Lines Complement Diagnostics of Massive-Star/ISM Interactions
  - ☞ ISM/Shock Interactions
  - ☞ Hot-Bubble Evolution
  - ☞ Matter Recycling
  - ☞ Star Formation History
  - ☞ ISM Morphology

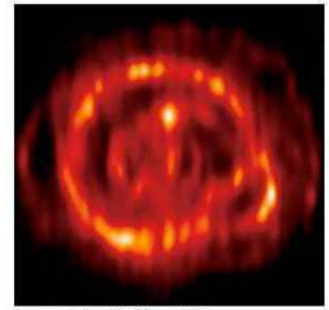

Face-on projection of the ISO map of M31.
(wavelength of 175 microns)

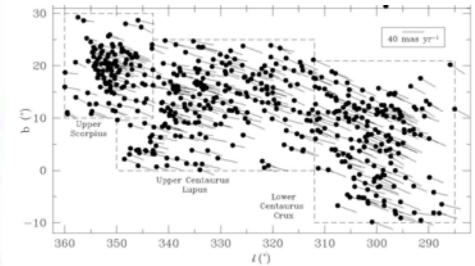

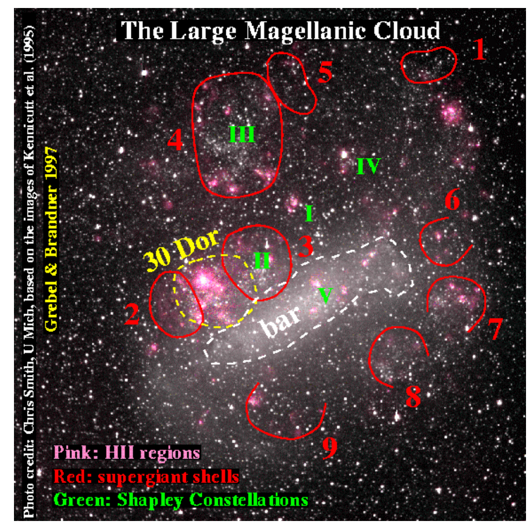

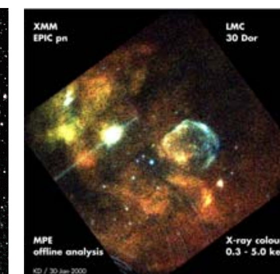

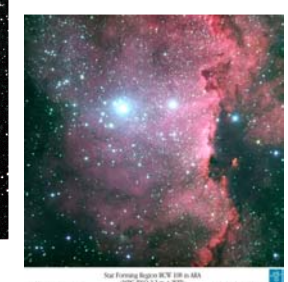

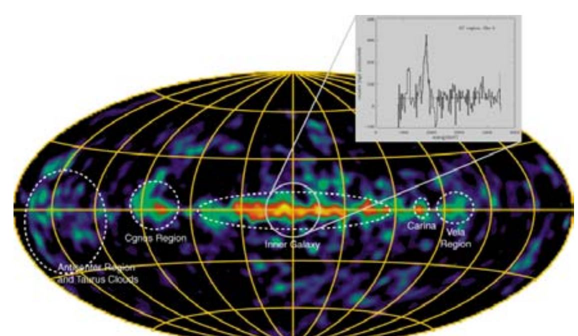

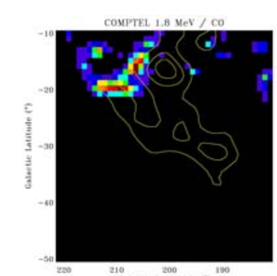

Roland Diehl